# PG&E's Composite Risk Model for Overhead Electric Transmission Components

PG&E Risk and Data Analytics Team

© 2025 Pacific Gas and Electric Company. All rights reserved.

# PG&E's Composite Risk Model for Overhead Electric Transmission Components

Prepared for: PG&E Risk and Data Analytics Team

Prepared by:

Exponent
149 Commonwealth Drive
Menlo Park, CA 94025

© Exponent, Inc.

# Contents

# List of Figures

# Definitions

Definitions used in risk assessments vary by industry and application. The definitions used herein are specific to this application and may differ from those used elsewhere.

***Annual Exceedance Frequency (AEF):*** The number of times, on average, a hazard intensity is exceeded in one year. AEF is the reciprocal of the mean return period of a hazard intensity.

***Annual Failure Rate*:** The expected number of unwanted outcomes (e.g., failures) in one year. It is the reciprocal of the mean time between failures (mtbf). For low annual failure rates (less than 0.02), it is approximately equal to the ***annual probability of failure***.

***Annual Probability of Failure*:** The probability of at least one unwanted outcome (e.g., failure) occurring in one year.

***Asset*:** The combination of a transmission line structure (e.g., a lattice tower or a wood pole) and all components supported by the structure (e.g., conductors, hardware and equipment).

***Component grouping:*** A group of components with similar lifecycle, sensitivity to threats/hazards, and asset management strategy.

***Composite Annual Probability of Failure*:** Annual probability of failure combined across multiple component groupings and/or multiple hazards.

***Degradation*:** Reduction in capacity, or increase in uncertainty, over time caused by a threat.

***Design Life:*** The theoretical age of a component or structure at which the uncertainty regarding whether it remains fit for purpose is so high (or, conversely, the confidence is so diminished) that it would be scheduled to be either replaced, hardened or re-certified based on engineering analysis.

***Expected Useful Life (EUL)*:** The age of a component or structure, based on average degradation rates and external hazards, at which the risk of failure outweighs the benefits of continued inspection, maintenance, repair and/or hardening.

***Failure (or Unwanted Outcome)*:** The inability of the asset to perform its expected function. Examples of failures could include support collapse, heat- or flood-induced equipment failure, clearance violation, or the inability to provide service due to any number of underlying causes.

***Failure Rate Tolerance (or Failure Rate Appetite)*:** A failure rate above which the risk associated with a component or asset is unacceptably high.

***Fragility*:** The conditional probability of an unwanted outcome given the intensity of a hazard (e.g., the likelihood of pole groundline failure given a peak wind gust of 100 mph).

***Fragility function:*** The locus of fragilities for all hazard intensities. Fragility functions are conventionally expressed as lognormal cumulative distribution functions defined by a median, $\mu$, corresponding to the median hazard intensity at which the unwanted outcome occurs, and a dispersion parameter, $\beta$, which defines the shape of the fragility function (i.e., the probabilities of unwanted outcomes corresponding to all hazard intensities).

***Hazard*:** An event that causes a failure or other unwanted outcome. Events can be external (environmental) or internal (design flaw, operation error, etc.). Examples of external hazards include wind loads, wildfire, and earthquake ground shaking.

***Hazard Curve*:** The locus of annual exceedance frequencies (or equivalently, mean return periods) for all hazard intensities. The term hazard is often used to describe the numerical value of the annual exceedance frequency at a particular intensity such as design level (e.g., 0.01 would be the hazard associated with the 100-year return period wind speed).

***Intensity:*** The measure of a particular hazard used to predict how the asset will perform and the probability of an unwanted outcome (e.g., the intensity measure for a wind hazard is typically the peak gust speed averaged over 3 seconds).

***Mean return period (MRP):*** The time, on average, between events of a given hazard intensity. MRP is the reciprocal of the annual exceedance frequency of a hazard intensity.

***Risk*:** The combined effect of probability of an unwanted outcome (failure) and the consequence (cost) of that outcome, considered in an overall context (e.g., failure during high wildfire threat conditions). In quantitative risk assessments, risk is often calculated by combining the hazard with fragility and the cost of consequences; costs are outside the scope of this report, but the framework herein is formulated so that it can be expanded to include probabilistic cost functions.

***Risk Integral*:** An equation used to determine an annual failure rate by combining the hazard and fragility functions in the context of the Total Probability Theorem. The risk integral can be

expanded to include probabilistic definitions of the cost and downtime, but those extensions are outside the current scope of the framework herein.

***Threat*:** A phenomenon that reduces an asset's ability to resist the effects of a hazard. Examples of threats include wood decay, steel corrosion, wear, and metal fatigue. A threat will typically affect the fragility such that, over time, the probability of an unwanted outcome (failure) increases for a given hazard intensity.

# 1. Architecture of the Transmission Composite Model

The fundamental purpose of the work described herein is to provide a scientifically sound framework by which Pacific Gas and Electric Company (PG&E) can incorporate asset health and site-specific hazards into their risk-informed overhead electric transmission asset management. This paper describes the technical basis for the framework, while the software that applies this model is referred to as the Composite Risk Tool. For convenience, and consistent with current parlance within PG&E, the framework and its software implementation are collectively referred to herein as the Transmission Composite Model (TCM).

The technical basis of this framework is often attributed to Dr. C. Allin Cornell's original research at M.I.T. and later work while at Stanford. The framework has been applied for decades to the quantitative seismic assessment of nuclear structures, and virtually all nuclear power plants and Department of Energy nuclear structures in the U.S. have been designed and assessed using these methods. More recently, the fundamental aspects of the framework have been adopted into more general structural engineering standards, and now form the basis of the seismic design provisions of building codes. Moreover, building codes now allow direct application of the method for building design as an alternative to the prescriptive requirements of the codes. This new design paradigm is termed Performance Based Engineering (PBE), and it is becoming more common. In fact, many new California high-rise buildings have been designed using PBE in lieu of the seismic design provisions of the building code. The framework described in this paper uses the principles of PBE to evaluate the risk to assets that suffer environmental degradation that, over time, reduces their ability to resist external hazards.

The framework is built upon a number of key underlying principles, described briefly here and in more detail in later sections:

- *Assets* are put to use in environments that are not benign, and asset health will degrade with time. The *degradation* of asset health is accompanied by an increase in the probability the asset will fail due to an external *hazard*. The probability of asset failure is a function of its original design, its current health, and the site-specific nature of the hazards (e.g., probabilities of failure are higher at windier sites).

- At some point in its life, an asset will have degraded to the degree that the probability of failure becomes unacceptably high. This point describes the end of its useful life; that is, the risk of failure outweighs the benefits of continued inspection, maintenance, repair, and/or hardening. An asset put into service has an *expected useful life* (EUL) based on average degradation rates and external hazards. For instance, wood poles may have an EUL of 60 years, though many poles in less aggressive environments can last much longer, and those in more aggressive environments might be replaced earlier (Figure 1).

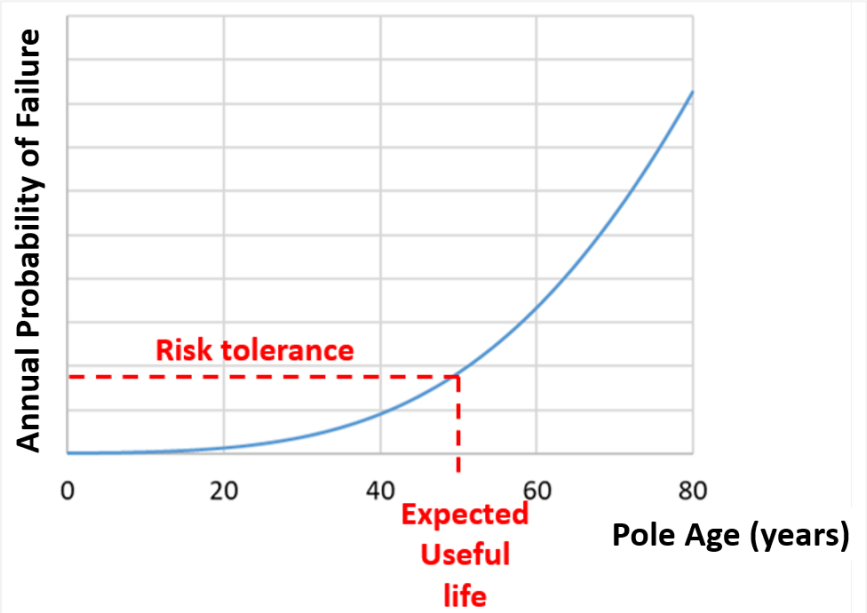


Figure 1. Increasing annual probability of failure with time, and its relation to useful life.

- One way to calculate the failure rate is by the *Risk Integral* (described in a subsequent section). The Risk Integral takes as input the asset health (in the form of a *fragility function*) and the likelihood of experiencing an extreme external load (in the form of a *hazard curve*). The Risk Integral can be evaluated based on projected future health as determinized by degradation models to determine the increase in failure rates with time and the end of useful life when the failure rate crosses an acceptance threshold or *failure rate tolerance*.

- Herein, we assume that the failure rate will increase with time due to degradation that begins at the time of installation. Readers familiar with the bathtub curve for product failure rates will note that this neglects early failure rates due to product design and manufacturing defects (the so-called infant mortality portion of the curve). High early failure rates from those causes are outside the scope of the current framework.

- The probability that an asset will fail at a given hazard intensity (e.g., wind speed or ground shaking acceleration) is termed *fragility*. Low hazard intensities result in low probabilities of failure, while high intensities increase that probability. As such, when *fragility functions* are plotted, they resemble an "S" curve, and are conventionally defined by lognormal cumulative distribution functions, which are defined by a median, $\mu$, corresponding to the median hazard intensity at which the unwanted outcome occurs, and a dispersion parameter, $\beta$, which defines the shape of the fragility function (i.e., the probabilities of unwanted outcomes corresponding to all hazard intensities).
- Fragility functions can evolve with time as an asset degrades. The underlying causes of the degradation mechanisms are referred to as *threats*. Threats could include fungal decay for wood poles or atmospheric corrosion for steel components. The degradation mechanisms associated with these threats are modeled to predict future fragility functions and associated failure rates.
- The likelihood that an asset will be subjected to an external load of a given intensity during a given time period is known as the site hazard, and is typically given in the form of a *hazard curve*. The notion of hazard curves is somewhat familiar because we use the phrase return period to describe the intensity of floods and windstorms. For instance, a 60-mph wind may have a mean return period of 50 years,[1] whereas a 90-mph wind may have a return period of 100 years. The locus of the return periods associated with all wind speeds forms a hazard curve. Hazard curves are conventionally expressed in terms of the reciprocal of the return period, which is termed the annual exceedance frequency (AEF), and are commonly fit to extreme value probability distributions, such as the Gumbel distribution for wind hazard.

For some assets and hazards, there is sufficient information regarding failure rates to preclude the need for evaluation of the Risk Integral, and it is more appropriate to simply estimate failure rates directly rather than model fragilities or hazards that may not be amenable to mathematical models. An example of this is vehicle impacts to transmission line structures, for which the hazard is not amenable to modeling, and direct modeling of the failure rates based on past impacts is more appropriate.

More detailed descriptions of the hazards, fragilities, threats, and failure rates are provided in the following sections.

[1] A wind with a mean return period of 50 years is exceeded, on average, once every 50 years.

## Limitations of the Framework

This report is a living document intended to record the continuous, teamwork-driven process of framework development based on input, recommendations, and guidance from diverse groups and subject-matter experts. The contents of this document should be considered the current, consensus view of the team rather than the opinions of the authors. As such, the contents of this document may change significantly throughout the course of the development of the framework, in both the long and short terms.

Exponent's work was undertaken to assist PG&E in their efforts to reduce the risk of future wildland fire ignitions from overhead electric transmission lines. The framework described herein is based on a diverse set of mostly qualitative data, which necessitates substantive simplifications and assumptions throughout. Although Exponent has exercised usual and customary care in the conduct of its work, it is understood and agreed that the responsibility for reviewing and implementing the framework described herein, including the incorporation of risk tolerances and recognition of the framework limitations, remains fully with PG&E. The framework underlying this work is based on mathematical and statistical modeling of physical systems limited to collection and processing of descriptions of the relative physical health of overhead transmission line assets. Given the nature of the underlying data, significant uncertainties are inherent, and any results from using this framework should be interpreted as indicators rather than facts or predictions of the behavior of specific assets or circuits. The actual performance of specific assets in extreme hazard conditions can be materially different than indicated by the framework.

# 2. Component Groupings and Assets

A PG&E Failure Mode and Effects Analysis (FMEA) in 2019 identified 47 critical transmission line components, such that a failure of a single component had the potential to result in a wildfire ignition. In 2021, a cross-functional team of subject-matter experts (SMEs) divided these components in *component groupings* based on similarities in lifecycle, sensitivity to threats/hazards, and asset management strategy.[2] This resulted in the following nine component groupings:

- Conductors
- Insulators
- Non-steel structures
- Steel structures
- Foundations
- Switches
- Above grade hardware
- Below grade hardware
- Splices

With the exception of switches, which are addressed by others, the framework described herein is applied to each of these component groupings. The failure rate estimated by the TCM for a component grouping is intended to conservatively estimate the failure rate for the most vulnerable component of the grouping.

At a given structure, the combination of the structure and all components supported by the structure is referred to herein as an *asset*. Failure rates estimated by the TCM for component groupings of an asset can be combined, resulting in an asset-level failure rate. This supports risk-informed asset management at the component grouping level (e.g., a program intended to address wildfire risk associated with wood pole failure) as well as at the asset level (e.g., enhanced inspection programs targeting high-risk assets).

[2] For a detailed discussion of the components and component groupings, see "Transmission Line Critical Component Grouping," dated September 7, 2021, by PG&E Transmission Line Asset Strategy.

# 3. Hazards

*Hazard curves* are used to quantify how frequently external hazards of various intensities will occur. For instance, consider points on a flood hazard curve representing 100, 200, 500, and 2500-year flood elevations; the locus of these points forms a hazard curve. These points are often fit to an extreme value statistical distribution such as Gumbel, as is done herein for wind hazards.

A hazard curve can take two equivalent forms, either showing the intensity as a function of annual exceedance frequency (AEF)[3] or its reciprocal Mean Return Period (MRP), as shown in Figure 2 and Figure 3, respectively. In the figures, the green curve represents a site with a lower hazard than the site represented by the red curve, as equal intensities have greater frequency (or equivalently shorter return periods) for the red curve. Given two identical assets, the asset located at the site represented by the red curve would experience higher rates of failure because of the higher hazard (higher frequency of intense loading). In this way, the failure rates calculated herein are site-specific.

The TCM currently considers hazards associated with wind and seismic loading; so-called third-party hazards associated with vehicle impacts, metallic balloons/kites, and gunshots/vandalism; and hazards associated with vegetation and avian impacts on a transmission line. Hazard curve formulations for each of these is described in the following subsections.

[3] In some instances, annual *probability* of exceedance is used rather than exceedance *rate*. For the hazard intensities of interest, this distinction will not have a measurable effect on calculated failure rates.

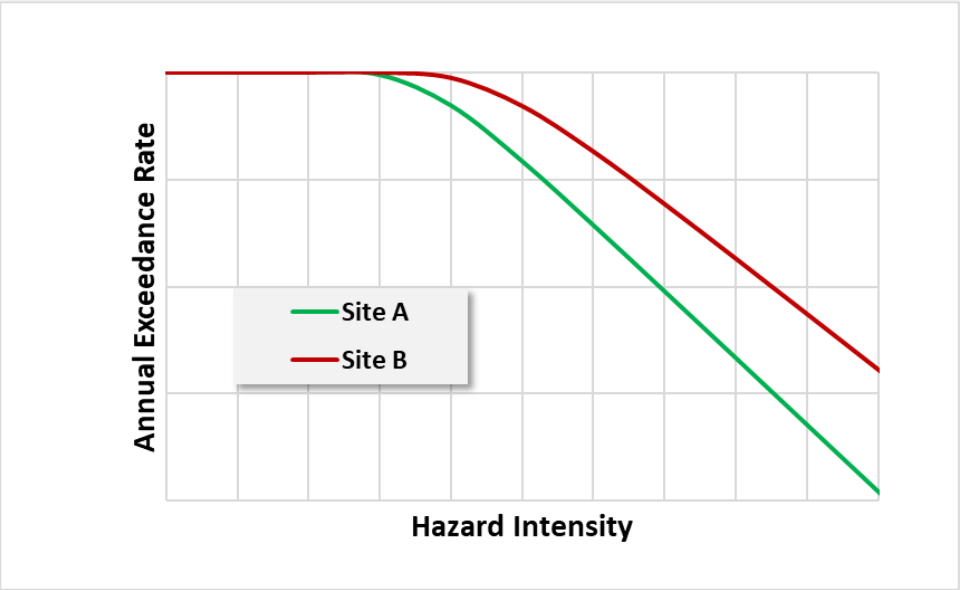


Figure 2. Generic hazard curve showing hazard intensity versus annual exceedance frequency.

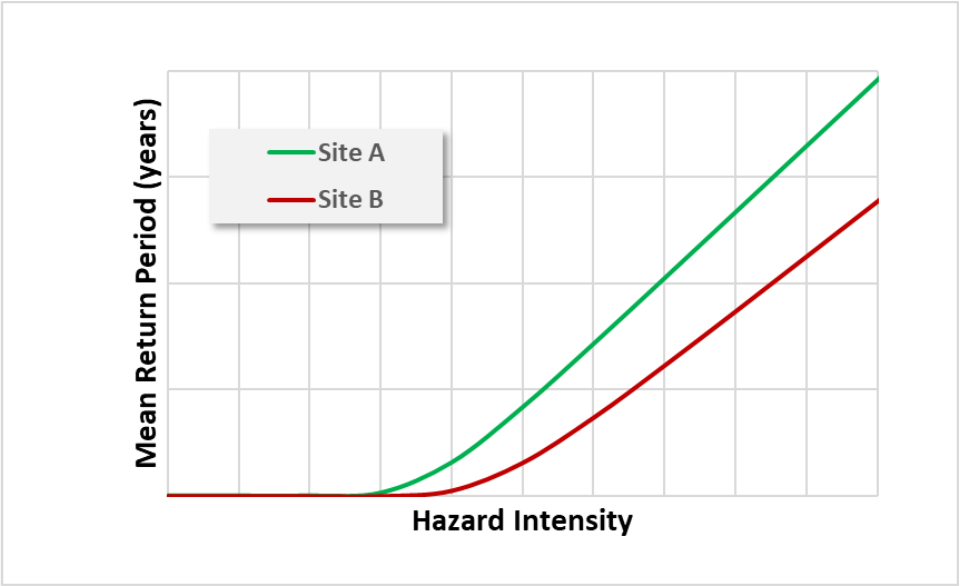


Figure 3. Generic hazard curve showing hazard intensity versus mean return period.

## Wind Hazard

The annual failure rates and useful life for many assets are defined by their ability to resist wind loads. As such, expected failure rates for many assets are calculated based on wind hazard, though the threats (degradation) come from multiple sources. In California, the minimum strength requirements for utility structures are prescribed by General Order 95 (G.O. 95), although California utilities may design to internal standards that exceed G.O. 95 requirements.

The wind hazard for assets considered herein are site-specific, based on meteorological data provided by PG&E. The data is provided for the entire service area on a 2 km × 2 km grid and is based on over 30 years[4] of data collection and modeling of maximum hourly wind each day, converted to 3-second gust equivalent. Data provided includes ordered pairs of wind speed and the percentage of days over the time period of record for which the speed was not exceeded (i.e., the maximum recorded wind speed was lower than the given speed).[5] For example, a pair of 40 mph and 60% would indicate that, at this site, on 60% of the days the maximum wind speed was lower than 40 mph. This empirical wind data is fit to an Extreme Value Type I (Gumbel) distribution by determining the Gumbel location and scale factors that minimize the error in the percentiles for all wind speeds weighted equally (Figure 4). The percentiles associated with the fit allow direct calculation of mean return periods and annual exceedance frequencies (Figure 5),[6] which are used in the failure rate calculations.

The resulting wind speed maps for the PG&E service area showing the 50, 100, and 150-year mean return period 3-second gusts appear in Figure 6, Figure 7, and Figure 8, respectively.

---

[4] The meteorological data extends back to 1989.

[5] The data records the highest wind speed regardless of direction. Herein, we make the conservative assumption that the wind comes from the most adverse direction for each asset.

[6] Note that the annual exceedance frequency of the lowest recorded wind speed from the dataset will be 365 since that wind speed was exceeded on every day of every year.

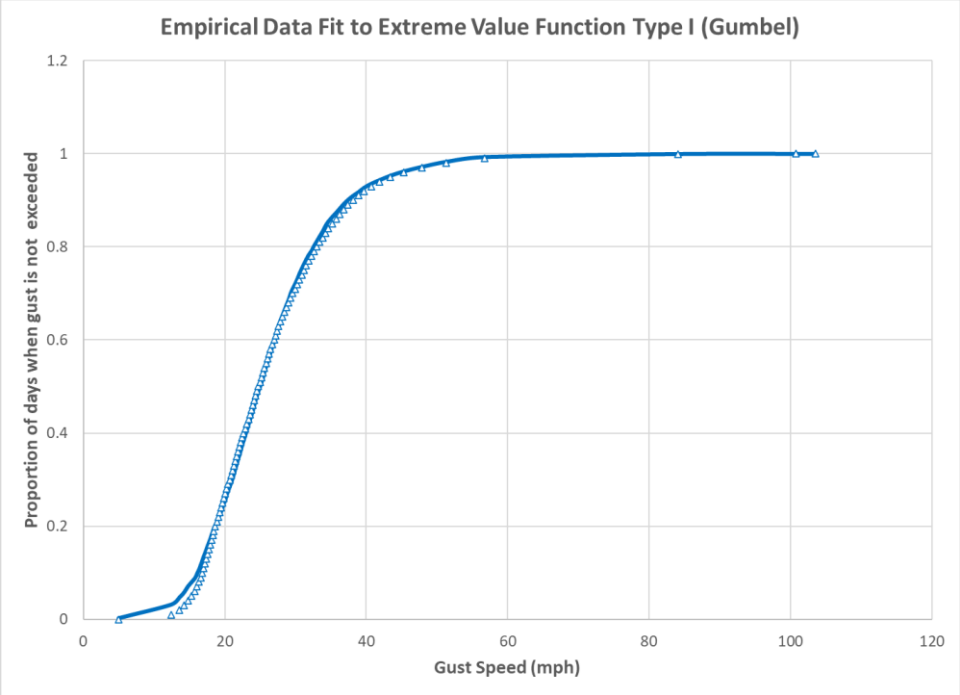


Figure 4. Example of Gumbel distribution fit to PG&E wind percentiles.

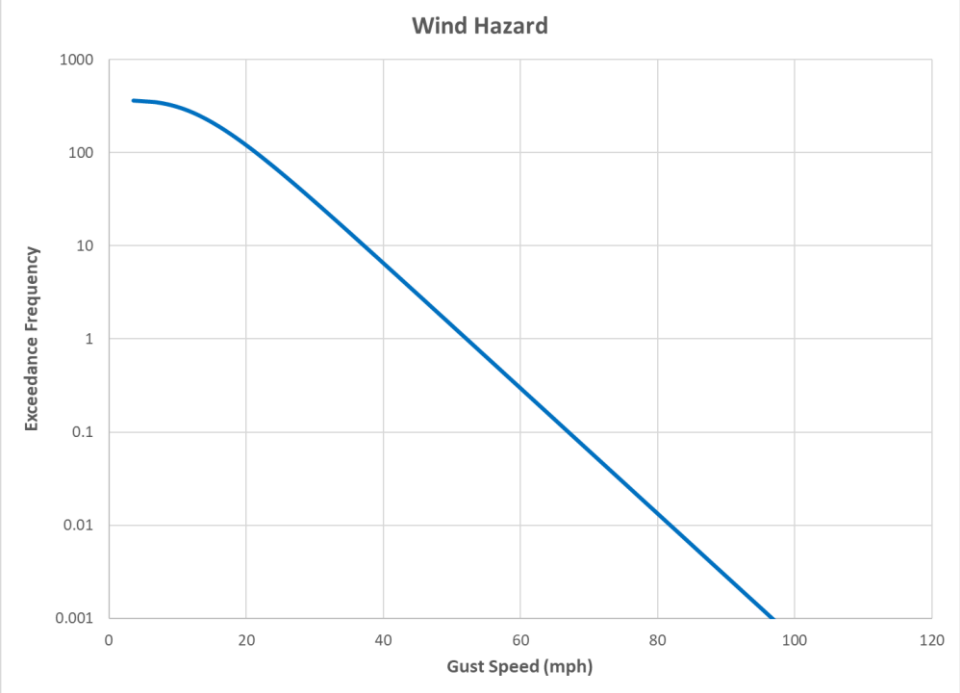


Figure 5. Wind hazard curve based on fit shown in Figure 4.

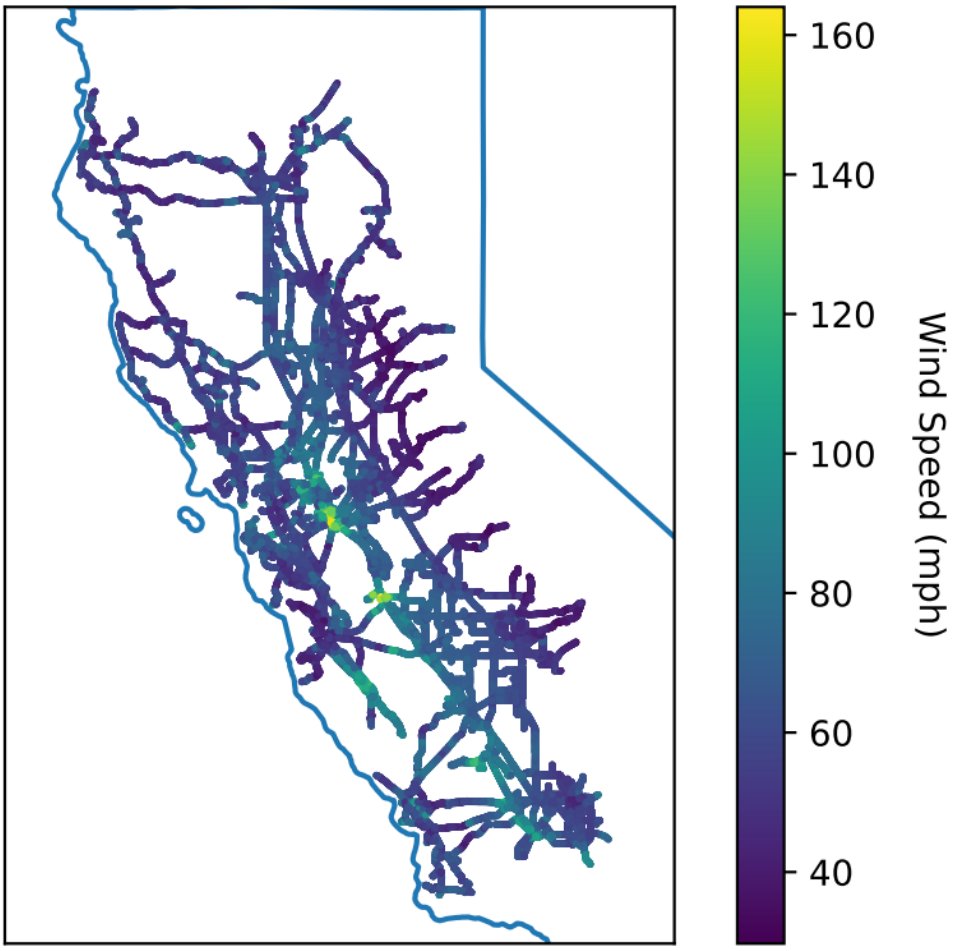


Figure 6. 50-year mean return period 3-second gust speed mapped at each transmission structure.

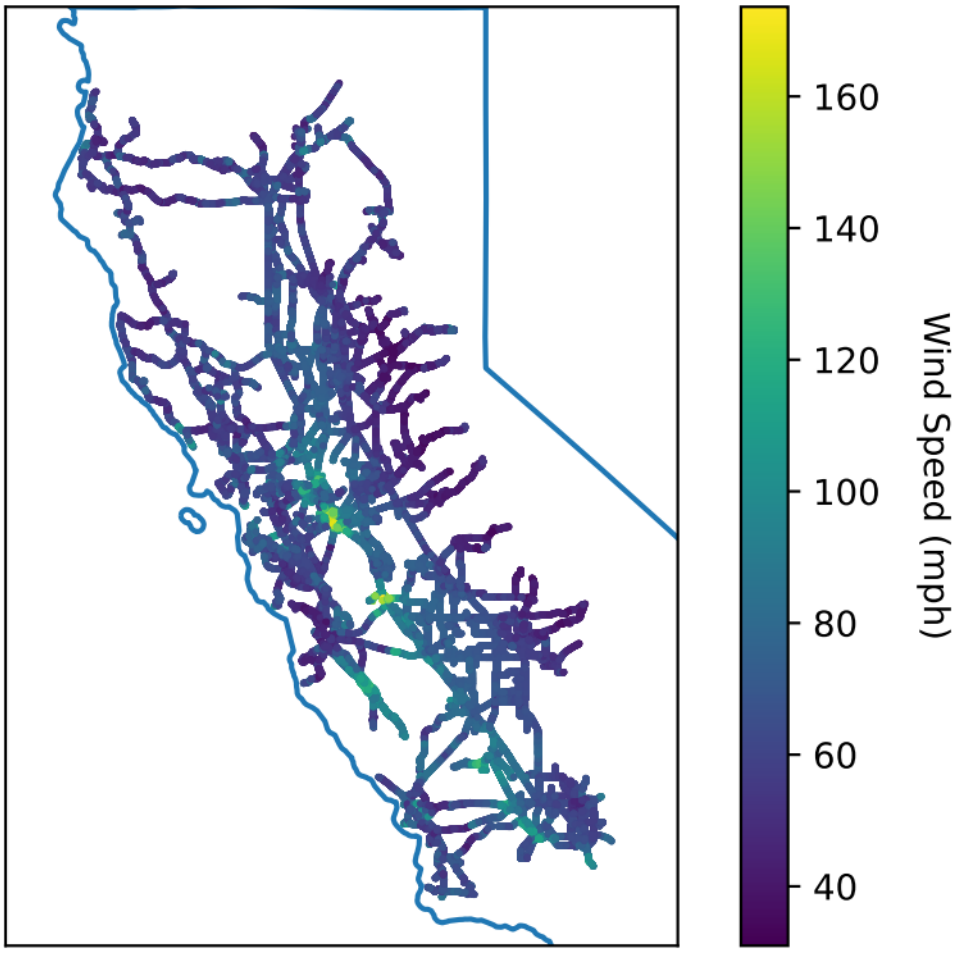


Figure 7. 100-year mean return period 3-second gust speed at each transmission structure.

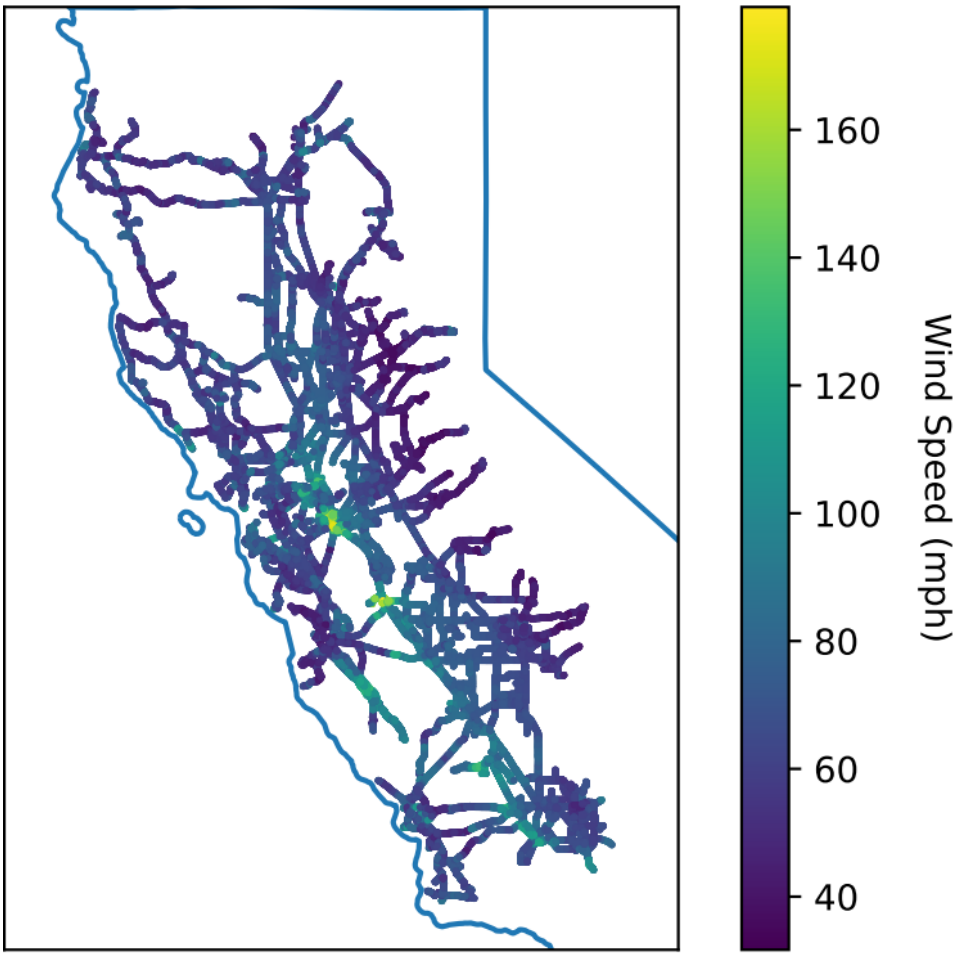


Figure 8. 150-year mean return period 3-second gust speed at each transmission structure.

Figure 9 shows a histogram of the 100-year mean return period wind speed at each structure location. The substantial variability across the PG&E service territory is an indication of how important it is to consider the wind environment when risk-ranking similar assets.

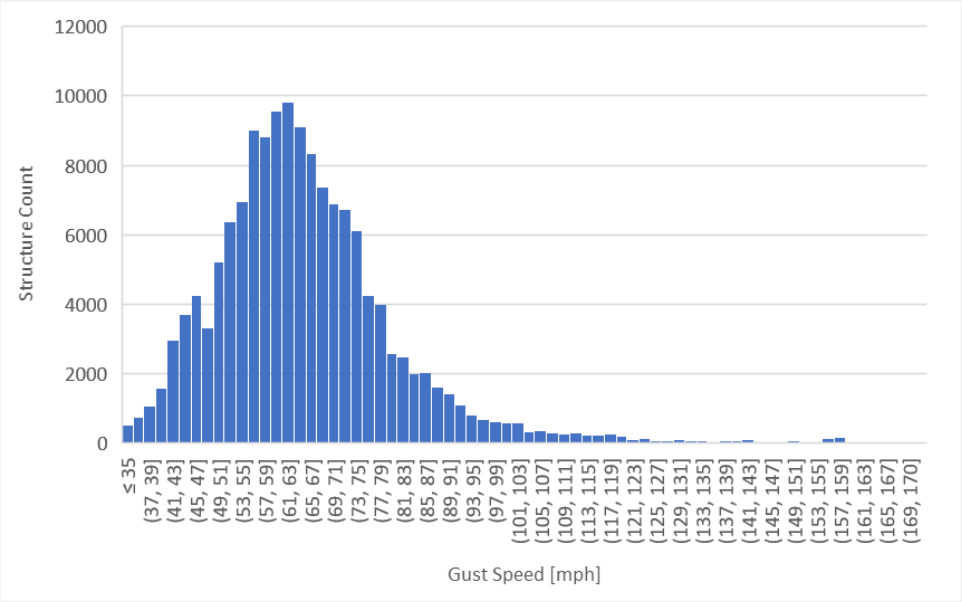


Figure 9. Histogram of 100-year mean return period winds for all structures.

## Seismic Hazard

The TCM estimates annual probabilities of failure of wood poles and steel transmission towers due to inertial forces and landslides. For the inertial force models, peak ground acceleration (PGA) is used as the intensity measure for wood poles because they are expected to be relatively rigid, while spectral acceleration at the first mode period, Sa(T1), is used for steel towers due to the potential for flexibility of the towers. The first mode period of several transmission tower types was calculated by performing a modal analysis of the towers. Site-specific hazard curves for both PGA and Sa(T1) are taken from the USGS 2018 dynamic conterminous model based on the soil site class at each location. These hazard curves are integrated with fragility curves to determine the annual failure probabilities of wood poles and steel towers due to inertial forces.

The landslide analysis uses the joint probability distribution of PGA and earthquake moment magnitude (M) as its intensity measures because expected landslide displacements, which are used to determine failure probabilities, are a function of both PGA and M. The joint probability distribution is determined from the USGS 2018 dynamic conterminous model at numerous return periods such that a hazard curve for PGA can be defined, and the distribution of M at

each PGA intensity level on the hazard curve is also defined. This enables probabilistic estimates of landslide displacement hazard curves that consider jointly distributed intensity measures.

For a detailed description of the seismic hazard data used by the TCM, see Appendix A, which includes information related to the following component/hazard combinations:

- Wood pole inertial force
- Steel tower inertial force
- Wood pole landslide (in progress)
- Steel tower landslide (in progress)

## Hazards for which Failure Rates are Otherwise Estimated

There are some external events that can cause failures or outages that are not amenable to hazard curve formulation or failure rate calculation using the Risk Integral. Failure rates from these hazards are modeled directly based on past performance, SME input, and engineering judgment. Such hazards are described below.

### Third-Party Hazards

The TCM currently considers third-party hazards associated with vehicle impacts, metallic balloons/kites, and gunshots/vandalism. Annual probabilities of the occurrence of damage events caused by these hazards were estimated by Urbint using machine learning models that ingest work order, outage, and inspection data related to each hazard. Probabilities were provided for hexagonal grid cells throughout the PG&E service territory.[7]

Because the TCM estimates failure rates at the asset and component grouping levels, results from the third-party hazard models are apportioned to the relevant assets and component groupings so that the results can be combined with those of other hazards. For car impact

[7] Results provided by Urbint represent the annual probability of at least one damage event associated with the hazard of interest within the grid cell. For purposes of the TCM, a third-party damage event is considered equivalent to a failure due to one of the other hazards (e.g., wind). In other words, annual probability of at least one damage event is considered equivalent to annual probability of failure.

hazard, probabilities of damage events are apportioned equally to the structure component groupings (steel structure or non-steel structure) of all assets in a hexagonal grid cell. For metallic balloon/kite hazard, probabilities of damage events are apportioned equally to the conductor component groupings of all assets in a hexagonal grid cell. For gunshot/vandalism hazard, probabilities of damage events are apportioned equally to the conductor and insulator component groupings of all assets in a hexagonal grid cell.

According to Urbint, results from their third-party hazard models are intended to be evaluated at the hexagonal grid level, and results have been apportioned to relevant themes and component groupings in the TCM solely for the purpose of combining with results associated with other hazards. See documentation by Urbint for details regarding their third-party hazard models.

## Vegetation and Avian Hazard

Annual rates of outages associated with vegetation- and avian-related causes were estimated by PG&E using machine learning models trained on historical outages for transmission lines compiled since 2007.[8] Similar to the third-party hazard models, the vegetation and avian hazard models were provided for hexagonal grid cells throughout the PG&E service territory, and results are apportioned to the relevant assets and component groupings. For both the vegetation and avian models, failure rates are apportioned equally to the structure (steel structure or non-steel structure) and conductor component groupings of all assets in a hexagonal grid cell.

Documentation by PG&E for the vegetation and avian models implemented in the TCM is currently ongoing.

[8] "Wildfire transmission Risk Model (WTRM): Vegetation and Avian Hazard Risk Model, Version 1," by PG&E.

# 4. Fragility Functions

Transmission assets are designed to withstand various external (environmental) hazards, such as high winds and ice accretion. It is possible, based on engineering principles or past performance of similar assets, to estimate the capacity to resist each hazard (e.g., the wind speed at which we expect the pole to snap at its base). However, material properties and construction practices vary, and therefore the capacities of nominally identical assets will vary. Moreover, our engineering models are imprecise, and we cannot predict failure loads with 100% accuracy. As such, we can never know an asset's capacity to withstand a given hazard intensity with complete certainty. A benefit of using *fragility functions* is that both the asset's capacity as well as the degree of certainty with which it can be predicted are quantified and tracked.

Fragility functions quantify the probability of some unwanted outcome (failure)[9] given that the asset is subjected to a hazard of some intensity. For instance, the increasing probabilities that a wood pole will break at the ground line due to transverse wind could be estimated for peak gusts of 50, 100, and 200 mph. The locus of these points forms a fragility function that is conventionally expressed as a lognormal cumulative distribution function defined by a median, $\mu$, corresponding to the median hazard intensity at which the unwanted outcome occurs, and a dispersion parameter, $\beta$, which defines the shape of the fragility function (i.e., the probabilities of unwanted outcomes corresponding to all hazard intensities).[10]

The fragility functions for new component groupings in the TCM subjected to wind hazard are derived from publicly available technical literature describing reliability studies of electric transmission structures. The basis for new metallic components was obtained from the document *Reliability-Based Design of Transmission Line Structures: Final Report*, Publication EL-4793 by the Electric Power Research Institute. Based on calibration studies, that document

[9] Failure is put in quotes here because it is the common terminology in quantitative risk assessments, even when the outcome is not a failure in the usual sense (collapse or broken component). Fragility can represent the probability of exceeding any limit state, such as noncompliance with standards or the onset of a condition that requires further inspection.

[10] The median strength, by definition, is the wind speed at which half of the assets would be expected to fail. The dispersion represents the uncertainty in our strength estimation and is reflected in the width of the bell-shaped curve of the probability distribution.

recommends that utilities developing new design standards for lattice transmission structures target a reliability (annual probability of failure) of $2.7\times10^{-5}$ (based on a 50-year reliability index of 3.0). The basis for new wood and polymer components was obtained from the document *Reliability-based Design of Utility Pole Structures*, a 2006 publication by ASCE, which suggests a higher annual probability of failure of $4.6\times10^{-4}$ (based on a 50-year reliability index of 2.0) for existing wood poles. Based on technical literature and engineering judgement, values for the standard deviation of the natural logarithms of strength for new metallic and wood/polymer component groupings are taken as 0.2 and 0.3, respectively. The corresponding new component grouping fragilities based on these calibration studies are shown in Figure 10.[11]

The calibrated fragility functions described above assume all component groupings have been sized/selected based on the minimum design wind loads for transmission structures. This assumption is in the process of being refined by computer-aided structural analyses by others, using the software PLSCADD. While PLSCADD results are available for only a limited number of assets at this time, the median strength parameter of the fragility functions is adjusted for component groupings where results are available.[12] Fragility functions have also been adjusted based on past outage performance of the component groupings along each transmission line using a statistical model based on Bayesian inference and current asset health as reflected in

[11] For a more detailed description of fragility curve development, see *A Framework for Risk-Based Transmission Line Asset Management and Operability Assessment, Revision 7*, by Exponent, dated January 13, 2023.

[12] Where PLSCADD results indicate a component grouping has been "overdesigned" with respect to the minimum design wind loads, the median of the fragility function is increased, and vice versa. To account for the possibility of failure modes not analyzed by PLSCADD, the increase in the fragility is capped at a value associated with doubling the minimum wind-related design strength.

open repair tags assigned to the component groupings.[13, 14, 15] These adjustments are reflected in the "multi-feature" mode of the various TCM user displays, while results without these adjustments are reflected in the "threat-only" mode. The relevant mode of the TCM should be determined by the user, depending on the intended application.

Fragility functions are typically not constant over time, but will evolve as the asset degrades. For instance, wood poles can be weakened by fungal decay, or metallic conductors can be weakened by small fatigue cracks due to Aeolian vibration. The threats to different asset types and modeling of the degradation mechanisms are described in the next section.

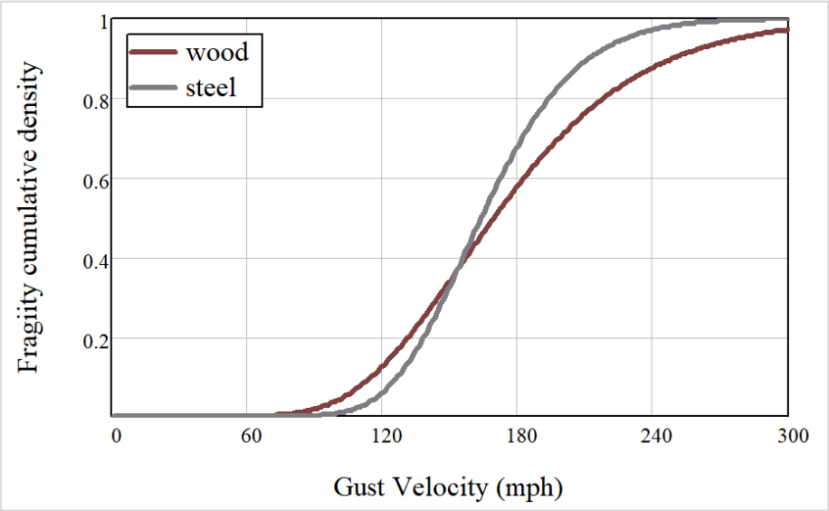


Figure 10. Fragilities for metallic and wood/polymer component groupings with median strength based on EPRI and ASCE calibration studies, respectively.

[13] For a more detailed description of fragility curve adjustments, see *A Framework for Risk-Based Transmission Line Asset Management and Operability Assessment, Revision 7*, by Exponent, dated January 13, 2023.

[14] As of the date of the current report, the statistical model of the Operability Assessment framework is applied at the asset level while that of the TCM is applied at the component grouping level (e.g., fragility functions for wood poles are not affected by outages caused by conductors in the TCM). It is anticipated that this enhancement of the TCM will be incorporated into a future version of the Operability Assessment model.

[15] Fragility adjustments in the current version of the TCM for damage identified by inspections are based on repair tags instead of condition codes (as is currently the case for the Operability Assessment model): a standard E tag results in a strength reduction equivalent to a condition code of 3 (1/3 strength reduction), a short-duration E tag to a condition code of 4 (1/2 strength reduction), and an F tag or cancelled S5 tag to a condition code of 2 (11/12 strength reduction). While an A tag would be equivalent to a condition code of 5 (2/3 strength reduction), these are typically addressed on an emergency basis, so their effect on annual estimates of probability of failure is considered negligible; A tags are therefore not used for fragility function adjustments in the TCM. It is anticipated that this enhancement of the TCM will be incorporated into a future version of the Operability Assessment model.

While overhead electric transmission and distribution assets are typically not designed for seismic hazard,[16] inertial forces imparted to these assets during an earthquake are similar in nature to lateral forces caused by wind. In the same way, the threats that weaken an asset relative to wind hazard also weaken the asset relative to seismic (inertial) hazard. For this reason, the fragility functions for new component groupings in the TCM subject to seismic (inertial) hazard are derived from calibrated wind fragility functions as detailed in Appendix A.

[16] G.O. 95 Rule 43 specifies temperature, wind, ice and dead weight as the loads to be considered in the design of components and structures.

# 5. Threats

In this framework, externalities that affect the fragilities over time are referred to as *threats*. Either decreased capacity (median strength) or increased uncertainty (dispersion) will cause the probability of failure for a given hazard intensity of interest to increase, thereby increasing the risk associated with that asset. For instance, wood poles can decay over time, thus reducing their structural capacity. However, we lose confidence in a wood pole's capacity to resist wind as the pole approaches the end of its design life, even if it is in visually good condition. Strength reduction shifts the bell curve model of capacity to the left, and increased uncertainty (higher standard deviation) causes it to fatten. As an example, consider the results of strength tests of new and existing poles conducted by the Electric Power Research Institute in the 1980s (Figure 11). The strength distribution of older wood poles has shifted the bell curve to the left, while increased variability (uncertainty) is illustrated by the fattening of the curve.

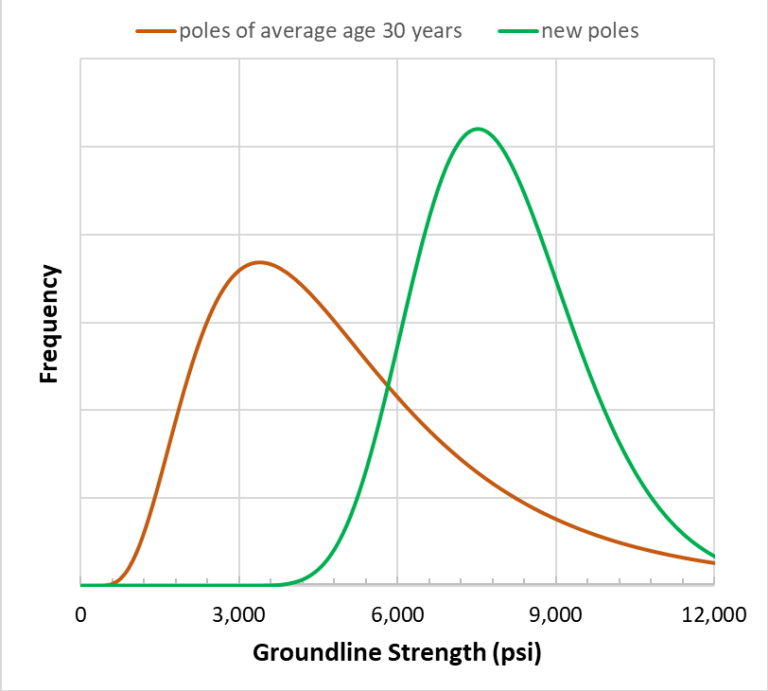


Figure 11. Loss of strength and increased dispersion as wood poles age[17] and the effect on fragility.

[17] Reliability-Based Design of Transmission Line Structures: Final Report, Publication EL-4793 by the Electric Power Research Institute, 1986.

## Effects of Decreased Capacity or Increased Uncertainty

This section describes the modeling of changes to both capacity and uncertainty due to the effects of external threats.

### Decreased Capacity[18]

Unless the asset is in a perfectly benign environment and made of indefatigable material, the asset's fragility function will change with time in ways that reflect an increased probability of asset failure. Consider the wind fragility function for groundline bending failure of an existing wood pole (Figure 12, black curve); in a 100-mph wind there is less than 5% chance of failure. If the base of the pole is subject to the *threat* of decay, in time its capacity to resist wind will be reduced. In this example, after 30 years, the probability of failure in a 100-mph wind increases from less than 5% to almost 40% due to the weakened base. The effect of this weakening on the fragility function can be seen as the dashed red curve in Figure 12.

[18] Capacity is defined as the asset's ability to perform its intended function in the presence of a hazard(s) of some intensity. In the current context of the TCM, it typically refers to physical strength, but in other contexts it could refer more generally to things like maintaining clearance to avoid flashover or maintaining the ability to deliver power.

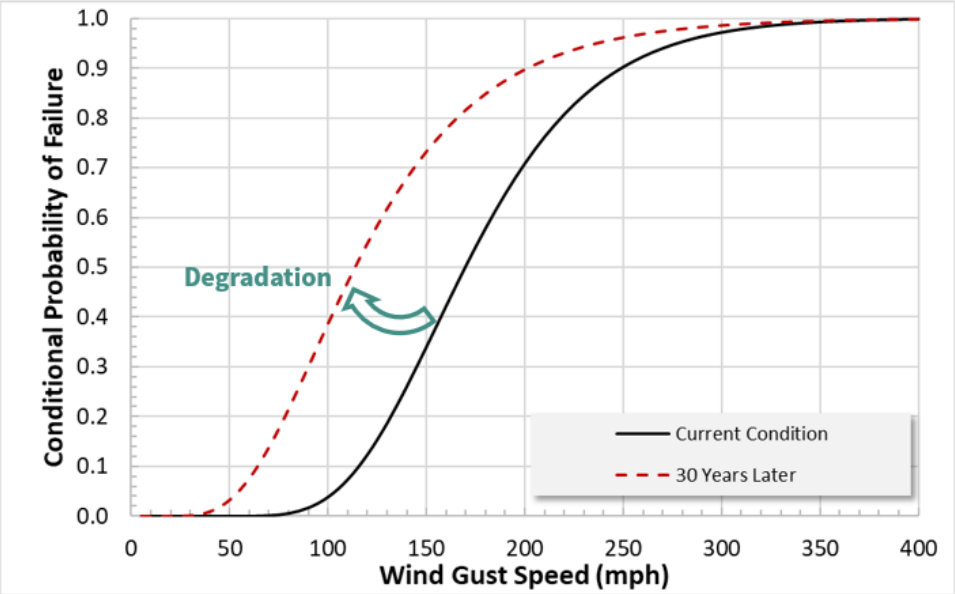


Figure 12. Fragility functions for an existing wood pole (black) and an aged, degraded pole (red dash).

## Increased Uncertainty

As discussed above, increased uncertainty surrounding asset capacity can also affect the fragility function. Consider the case of a tower that is sited in an area of persistent steady winds transverse to the conductor span, that is, under the *threat* of fatigue due to Aeolian vibration. Further suppose that the fatigue damage location is concealed within a connection such that it is difficult to inspect. Thus, as the conductor ages, we will become less confident in its ability to resist load, even though there is no visible indication of strength loss. In this example, after 30 years, our estimate of the probability of failure in a 100-mph wind increases from less than 5% to 12% due to increased uncertainty with age. This effect can be seen as the dashed red curve in Figure 13, which is rotated clockwise relative to the black curve as a consequence of fattening the underlying bell curve.[19]

[19] Counterintuitively, increased uncertainty results in *reduced* probability of failure at hazard intensities greater than the median, based on the standard lognormal formulation for fragility functions. For practical purposes, this has little impact on most risk models since the hazard intensities of interest are generally lower than the median. For the example shown in Figure 13, the median wind speed of approximately 170 mph is too high to contribute meaningfully to annual estimates of probability of failure for most sites.

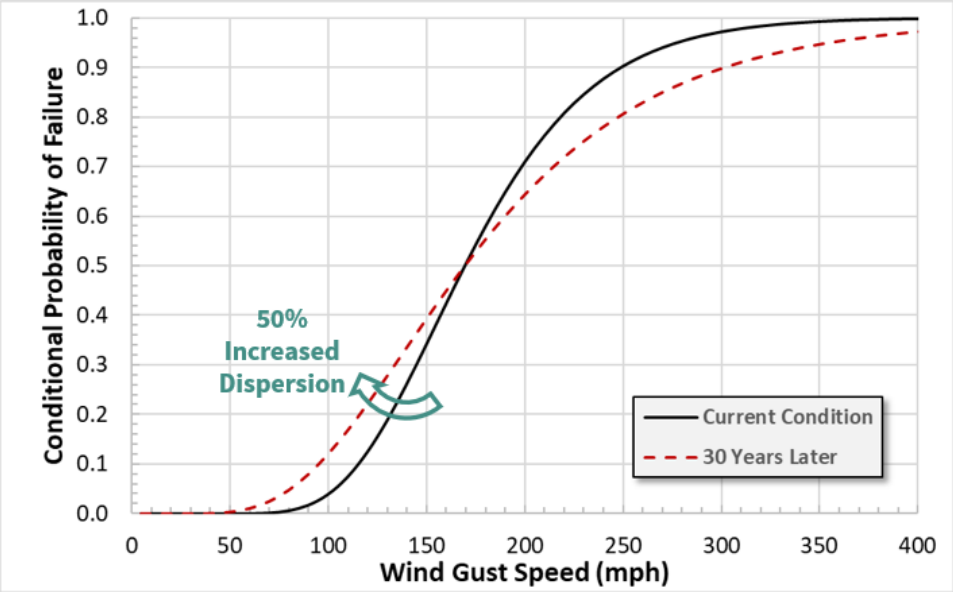


Figure 13. Fragility functions for an existing conductor span (black) and an aged conductor that exhibits no visible degradation (red dash).

## Design Life and Design Life Reduction Factors

One of the fundamental concepts used in the framework to track uncertainty is the notion that uncertainty increases with the age of the component, or put differently, we have less confidence in the behavior of older components compared to newer ones. There are two reasons for closely linking uncertainty and age. First, there may be degradation occurring that is not visible and that we cannot easily identify using currently available inspection tools and techniques, such as fatigue damage to a conductor concealed within a connection. Second, design standards and material specifications are presumed to continually improve with time, and newer components or structures should be better fit for purpose with more predictable capacities.

Another fundamental concept used in the framework is that the rate at which uncertainty grows also increases with age. In other words, our confidence in a component does not decrease as quickly in the first third of its design life as it does in the last third. Early in the design life of a component, this assumption is contrary to the so-called bathtub curve often used in product reliability studies, in which there is an increased rate of failure early in the life of a product due to design or manufacturing errors. Given the age of the existing transmission line structure stock, it was decided that the early life portion of the bathtub curve had passed for the vast

majority of components and that its inclusion would not meaningfully affect the framework results.

The third fundamental concept used in the Framework to address age-related uncertainty is the notion of a design life $t_D$. The design life is defined herein as the theoretical age of the component or structure at which the uncertainty regarding whether it remains fit for purpose is so high (or, conversely, the confidence is so diminished) that it would be scheduled to be either replaced, hardened or re-certified based on engineering analysis. This defines an important anchor point for our quantification of uncertainty: At $t_D$, the dispersion of the median strength (as a surrogate for fitness) has increased such that the associated probability of failure when subject to 8 psf wind pressure equals that which would result from a *strength* reduction of 1/3, absent any change in the uncertainty. The 1/3 strength reduction comes from G.O. 95 and is the strength degradation at which repair or reinforcement is mandated,[20] and 8 psf is the design wind pressure for light loading (no ice accretion).

As discussed above, the engineering parameter used in the framework to quantify the uncertainty is $\beta$, which is the standard deviation of the natural logarithms of the strength of a component grouping. Age of the component grouping is currently taken from PG&E's GIS data for the components of a particular component grouping, supplemented with conservative age logic[21] for component groupings without available GIS data. To represent the accelerated rate of uncertainty increase with age, a quadratic uncertainty-versus-age curve is assumed. The quadratic form is adopted because it is simple and exhibits the desired general shape; it is not based on first principles. The quadratic uncertainty curve is anchored at two points (and assumed to have zero slope at time zero):

- At $t = 0$, the dispersion is taken as $\beta = \beta_0$, which is the assumed strength dispersion for new construction based on technical literature and engineering judgement. The values of $\beta_0$ for metallic and wood/polymer component groupings are currently taken as 0.2 and 0.3, respectively.

[20] G.O. 95 Rule 44.3 requires replacement or reinforcement of components when safety factors have been reduced to less than two-thirds of the safety factors associated with new design.

[21] For a description of this logic, see "T-Line Asset Data Quality Improvement – Critical Components, Guide to Conservative Assumptions," dated January 14, 2020, by PG&E and GTS.

- The second anchor point is at a presumed design life $t_D$, at which we set $\beta = \beta_R$ such that it results in the same probability of failure subject to 8 psf wind pressure as would a strength reduction of 1/3, all else being equal.

Those three conditions, $\beta_0 = 0.2$ or 0.3 at $t = 0$; $\beta = \beta_R$ at $t = t_D$; and slope = 0 at $t = 0$, are sufficient to solve for the three coefficients of the quadratic form.

The Framework allows for increased uncertainty associated with an aggressive environment by shortening the presumed design life. Reduced design life causes the uncertainty to increase more quickly to $\beta_R$ thereby increasing the probability of failure at intensities of interest in a shorter time. Based on engineering judgement and review of age information for components across the PG&E network, the TCM currently uses a presumed "no threat" design life of 150 years for all component groupings with the exception of insulators, for which a presumed "no threat" design life of 100 years in used based on the results of a technical literature review suggesting more frequent replacement of insulators relative to other component groupings. This design life is a theoretical value for an asset in a perfectly benign environment, and should not be confused with actual useful life for a given component.

Threats can accelerate the increase in uncertainty with time through the use of a "design life reduction factor" (DLRF). In other words, a threat will cause the uncertainty of a component grouping to increase to a given level more quickly than an otherwise identical component grouping that is not subject to the threat. Figure 14 presents graphically the increase in uncertainty with time, including the effect of a DLRF.

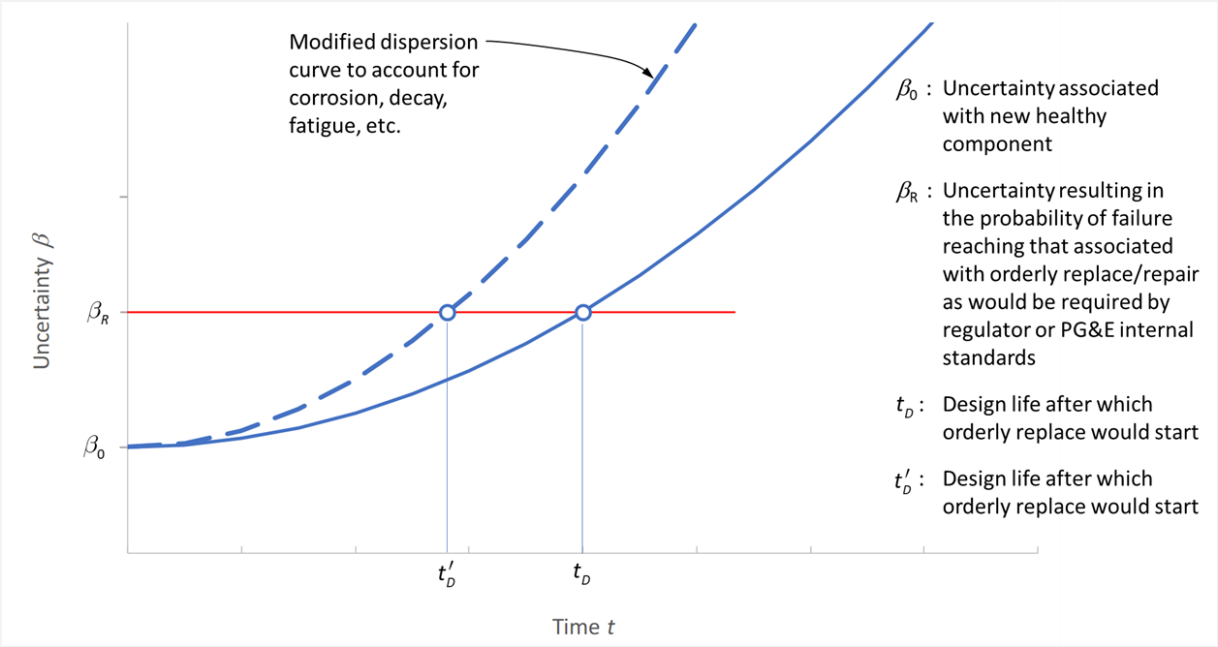


Figure 14. Model of uncertainty increase with time, and the effect on the rate of increase in the uncertainty with shortening the design life.

Currently, based on engineering judgement, the maximum DLRF applied for any single threat in the TCM is 1/3 the notional design life of the component grouping, with the exception of polymer insulators for which a maximum DLRF of 0.74 was calculated using the methodology described in Appendix I. The effects of multiple DLRF's for a single component grouping are combined by the square root of the sum of the squares method. For example, a component grouping with a DLRF of 1/3 for both corrosion and fatigue would have an overall design life reduction of $\sqrt{(1/3)^2 + (1/3)^2} = 0.47$.

In summary, fragility measures the health of an asset considering both its median strength and the uncertainty in our ability to predict that strength. The fragility of an asset subject to various threats will evolve with time: loss of capacity is demonstrated by a shift in the fragility curve to the left, while increased uncertainty is demonstrated by rotating the curve clockwise. Both of these effects increase the probability of failure at hazard intensities of interest.

## Specific Threat Models

Currently, the TCM includes the threat models shown in Table 1, which apply to the component groupings indicated in the table. Threats apply to wind and seismic (inertial) hazards, with the exception of insulator contamination, which applies to the hazard of critical moisture events.

Table 1. Threat model and component grouping matrix

| Threat Model | Component Grouping | | | | | | | |
|---|---|---|---|---|---|---|---|---|
| | Conductor | Insulator | Non-Steel Structure | Steel Structure | Foundation | Above Grade Hardware | Below Grade Hardware | Splice |
| Wood decay | | | ✓ | | | | | |
| Atmospheric corrosion | ✓ | ✓ | | ✓ | | ✓ | | ✓ |
| Underground corrosion | | | | | ✓ | | ✓ | |
| Fatigue | ✓ | | | | | ✓ | | |
| Wear | | | | | | ✓ | | |
| Insulator contamination | | ✓ | | | | | | |
| Poly insulator aging | | ✓ | | | | | | |

A summary of each threat model is included in the following subsections, with more detailed descriptions included in the referenced appendices.

## Wood Decay

**Relevant hazards:** wind, seismic (inertial)

**Relevant component groupings:** non-steel structure

**Effect on fragility function:** reduction in median strength, increased uncertainty (Cellon treatment)

The principal threat to wood poles is fungal decay, and wood pole replacement or hardening is most often due to strength loss from fungal decay (Figure 15). Decay reduces the cross-section of a wood pole that is effective in resisting load, typically at or near the groundline but also where water can be trapped at crossarms or at the pole top. PG&E assesses the potential for decay through its Pole Test & Treat (PT&T) program, which involves field-testing of each pole on a nominal 10-year cycle. PT&T results include an effective circumference, which can be used to estimate current remaining groundline bending capacity to that of the pole when new. Both the literature and PT&T results indicate that a significant population of wood poles begins to decay several years after installation, while another significant population does not decay even after many decades.

The wood decay model used by the TCM adjusts the median strength of a wood pole's fragility function based on PT&T results for that pole. Depending on the date of the last PT&T results, the model predicts the remaining strength at current and future dates by estimating a decay rate from successive PT&T results, or in the case of a pole with only one PT&T inspection, guidance from the literature regarding how long after installation of the pole appreciable decay is likely to begin. In some cases, PG&E uses external reinforcement to restore the capacity of a weakened pole. Early versions of the TCM did not account for such reinforcement, so the wood decay model continued to penalize poles with decay irrespective of reinforcement. Based on discussion with PG&E SMEs, the current version of the TCM restores the remaining strength of a reinforced pole to 2/3 of its undecayed strength. This is consistent with the strength reduction assumed to correlate with a standard duration E tag.[22]

[22] Modeling assumptions related to reinforcement of wood poles are conservative by design and not intended to reflect compliance-related decisions associated with this issue.

For a detailed description of the wood decay model used by the TCM, see Appendix B.

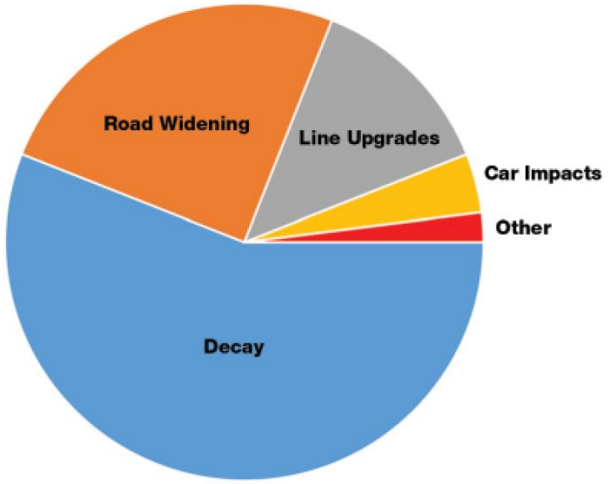


Figure 15. Reasons for pole removal.[23]

Poles are treated using various preservatives to inhibit decay. One of these preservatives, pentachlorophenol in liquified petroleum gas (referred to by its trade name *Cellon*), has been found to provide less effective treatment compared to other common preservatives.[24] Furthermore, decay of poles treated with Cellon often occurs just below the groundline and is therefore concealed to inspectors absent excavation or drilling down from the surface. A comparison of pole replacements by PG&E indicates a Cellon treated pole has a shorter expected useful life (EUL) than a pole with another treatment method. The TCM accounts for this difference in EUL by a DLRF of 33% for Cellon treated poles.[25]

For a detailed description of the effect of Cellon treatment on wood poles, see Appendix C.

---

[23] Morrell, Jeffrey, Estimated Service Life of Wood Utility Poles, North American Wood Pole Council Technical Bulletin No. 16-U-10, 2016.

[24] Based on discussion with PG&E SMEs, the following treatment names are treated as similar to Cellon for purposes of DLRF assignment: Butane, methane, propane, penta in liquid petroleum gas, and penta in chlorinated hydrocarbon solvent.

[25] Modeling assumptions related to gas treatment of wood poles are conservative by design and not intended to reflect compliance-related decisions associated with this issue.

## Atmospheric Corrosion

**Relevant hazards:** wind, seismic (inertial)

**Relevant component groupings:** conductor, insulator, steel structure, above-grade hardware, splice

**Effect on fragility function:** increased uncertainty

One of the principal threats to above-ground metallic components is atmospheric corrosion, which results in a loss of cross-section that is effective in resisting load. The rate of corrosion depends on environmental factors such as temperature, the presence of water on the surface of the component, and atmospheric pollutants. It also depends on the properties of the component, such as metal alloy, and the presence of paint or other protective coatings.

Systematic measurements of cross-section reduction associated with atmospheric corrosion are generally not available for PG&E components, and corrosion may occur at faying surfaces that are difficult to inspect. For these reasons, the adverse effect of atmospheric corrosion is modeled in the TCM as an increase in uncertainty (dispersion) of fragility functions for metallic component groupings. In other words, the useful life of a component in a highly corrosive environment is expected to be shorter than that of an otherwise identical component in a less corrosive environment.

For a detailed description of the atmospheric corrosion models used by the TCM, see Appendix D. Subsequent to the implementation of the atmospheric corrosion models in the early versions of the TCM, PG&E Applied Technology Services (ATS) performed ultrasonic thickness testing (UTT) measurements on tubular steel poles (TSPs) and light-duty steel poles (LDSPs) to obtain field estimates of wall loss due to corrosion.[26] Based on a comparison of these measurements with predictions by the atmospheric corrosion model of the TCM, it was determined that the TCM systematically overpredicted wall loss due to corrosion in TSPs and LDSPs. The agreement between field measurement and model prediction was improved by removing a calculation step in the model that effectively binned and maximized corrosion rates within a given corrosion category for conservatism. The field data demonstrated that this

[26] Because the interior portions of these cylindrical poles are inaccessible, UT measurements provide an estimate of current wall thickness that includes the effects of wall loss due to corrosion.

correction was no longer needed for these structure types. This modification for TSPs and LDSPs has been incorporated into the current version of the TCM. The modification was only applied for these structure types because similar UTT measurements are not available for other structure types and components.

## Underground Corrosion

**Relevant hazards:** wind, seismic (inertial)

**Relevant component groupings:** foundation, below-grade hardware

**Effect on fragility function:** increased uncertainty

One of the principal threats to below-ground metallic components is underground corrosion, which results in a loss of cross-section that is effective in resisting load. The rate of corrosion depends on environmental factors such as soil pH and the presence of groundwater. It also depends on the properties of the component, such as metal alloy and, in the case of foundations, the use of concrete to encase metallic components.

Systematic measurements of cross-section reduction associated with underground corrosion are generally not available for PG&E components, and the corrosion is typically concealed by soil. For these reasons, the adverse effect of underground corrosion is modeled in the TCM as an increase in uncertainty (dispersion) of fragility functions for metallic component groupings located below ground. In other words, the useful life of a component in a highly corrosive environment is expected to be shorter than that of an otherwise identical component in a less corrosive environment.

For a detailed description of the underground corrosion models used by the TCM, see Appendix E.

## Fatigue

**Relevant hazards:** wind

**Relevant component groupings:** conductor, above grade hardware

**Effect on fragility function:** increased uncertainty

Steady winds perpendicular to a conductor span cause vibrations due to vortex shedding, referred to as Aeolian vibrations. These high cycle, low amplitude vibrations can result in fatigue damage to conductors and the supporting hardware. The damage accumulates over time, reducing the capacity of the conductor and/or hardware. The occurrence of Aeolian vibrations depends on the wind environment, such as wind speed, direction and turbulence intensity. It also depends on properties of the conductor such as span length, span orientation, conductor type/size, and conductor tension.[27]

Fatigue damage may ultimately result in broken conductors or fractured connecting hardware. Advance detection of fatigue damage by visual inspection, however, can be difficult because the damage is often concentrated near the connection of the conductor and the hardware, and may therefore be concealed from view. For these reasons, the adverse effect of Aeolian vibration is modeled in the TCM as an increase in uncertainty (dispersion) of fragility functions for conductors and their associated above ground hardware. In other words, the useful life of a component with a configuration and in an environment prone to Aeolian vibrations is expected to be shorter than that of an otherwise identical component less prone to Aeolian vibrations.

For a detailed description of the Aeolian vibration model used by the TCM, see Appendix F.

## Mechanical Wear

**Relevant hazards:** wind

**Relevant component groupings:** above-grade hardware

**Effect on fragility function:** increased uncertainty

Wear is chiefly due to large deflections and associated rubbing when relatively light, unbraced components are buffeted in turbulent (gusting) wind. Damage associated with wear accumulates over time, reducing the capacity of hardware used to connect light, unbraced spans such as jumpers. The occurrence of wear depends on the wind environment, such as wind

[27] Conductor tension, a key determinant of a conductor's susceptibility to aeolian vibrations, is obtained from the results of PLSCADD modeling by others within PG&E (referred to as Method 1, or M1, models). In the current version of the TCM, tension values used to assess fatigue due to aeolian vibrations correspond to a temperature of 60 degrees F and were calculated using the ruling span convention for determining line tension. M1 data is currently limited to an annual refresh due to the annual refresh cycle of the supporting LiDAR data.

speed, wind direction and frequency content of the wind turbulence. It also depends on the properties of the components buffeted by the wind, such as mass, length, stiffness, and damping. Finally, wear depends on the thickness and material properties of the hardware components that are ultimately subject to material loss.

Currently, details regarding hardware and jumper components are not sufficiently available across the PG&E network to develop asset-specific structural models of the components. For this reason, Exponent's first-principles wear model assumes reasonable values for component properties relevant to the calculation of wear and applies site-specific wind properties to a structural model based on these reasonable values. The results of the wear model include the depth of wear for a typical metal hanger plate. For a detailed description of Exponent's first-principles wear model, see Appendix G.

The results of Exponent's first-principles wear model is used as an input parameter for a machine learning model by PG&E. This model is used to predict the likelihood of wear at assets throughout the PG&E network, sorted by PG&E into bins of high, medium, and low wear potential. These results are the basis of the DLRF for wear used in the TCM. See documentation by PG&E for details regarding the machine learning wear model.[28]

## Insulator Contamination

**Relevant hazards:** critical moisture event

**Relevant component groupings:** insulator

**Effect on fragility function:** increased probability of failure with accumulation

As contamination from dust, wildland fires, etc. accumulates on insulators, they become susceptible to flashover when a heavy fog or light rain occurs that generates ionized solution on the insulators. Over time, increased accumulation makes insulators more susceptible to flashover, while washing of the insulators from heavy rain removes the depositions and makes

[28] "Transmission Line: Above Grade Cold-end Hardware Mechanical Wear Model, Version 2 (MechWear-v2)," June 2023, by Sasha Yan (PG&E).

them less susceptible to flashover. Exponent has developed a first-principles model to calculate the annual rates of insulator flashover from this mechanism, as follows:

- Estimate the deposition rate of contaminants on insulators;
- Estimate the distribution of precipitation amount in a given period to determine the expected washing of the insulators;
- Estimate the rate that critical rainfall events occur, that is, heavy fog or light rain;
- Determine the relationship between the probability of flashover given a deposition total accumulation quantity and the voltage stress of the insulator, by insulator type, conditioned on the occurrence of a critical rainfall event;
- Simulate the accumulation of depositions, washing, and critical rainfall events to determine the rate of insulator flashover.

For a detailed description of the insulator contamination model used by the TCM, see Appendix H (in progress).

## Polymer Insulator Aging

**Relevant hazards:** wind

**Relevant component groupings:** insulator (polymer only)

**Effect on fragility function:** increased uncertainty

Polymer insulators experience a variety of environmental stresses throughout their service lives, which may lead to the reduction of their capacity to resist mechanical wind loads. The surface properties of polymer insulators may deteriorate under the effects of electrical stresses caused by corona discharge, leakage current, and/or arcing, which may be aggravated due to the presence of moisture and contaminants on the insulator surface. In addition to the risk of electrical failure addressed by the insulator contamination model, deterioration of the mechanical properties of the insulator surface may lead to exposure of the insulator core and mechanical failure. Exponent developed a statistical model to quantify the deterioration in the mechanical properties of polymer insulators based on their age in service and their location; the latter parameter affects the exposure of the polymer to environmental factors such as coastal

contamination and precipitation. The model is based on empirical observations of the degraded surface properties and mechanical strength of polymer insulators in various locations around the world. The model operates as follows:

- Available empirical evidence is used to develop a statistical relationship between the age and location of a polymer insulator and the corresponding deterioration of the surface properties of the insulator protective housing unit.
- A critical threshold for mechanical strength is defined based on severe deterioration of the protective housing and possible exposure of the insulator core to the environment.
- The statistical model estimates the useful mechanical service life of the insulator, which is defined as the age at which the insulator is predicted to reach the critical threshold for mechanical strength and varies based on its location.
- The estimated mechanical service life of the insulator is used to calculate a location-based DLRF for each polymer insulator location.

For a detailed description of the polymer insulator aging model used by the TCM, see Appendix I.

# 6. The Risk Integral and Projected Failure Rates

The hazard and fragility functions can be combined to calculate the annual rate $\lambda$ at which the unwanted outcomes will occur (i.e., the frequency at which the limit state will be exceeded, or failure rate for short). This equation is known as the *Risk Integral*. For low exceedance frequencies, the annual rate $\lambda$ approximates the annual probability of failure; annual exceedance frequency, annual failure rate, and annual probability of failure are often used synonymously in this context. This is not technically correct but is normally very close for practical ranges of failure probabilities. For example, for annual failure rates less than 0.02, the difference between the annual failure rate and annual probability of failure is less than 1%, assuming failures follow a Poisson process.

The Risk Integral is:

$$\lambda = \int_0^\infty p(f|im) \left|\frac{\mathrm{d}h}{\mathrm{d}im}\right| \mathrm{d}im$$

Where $p(f|im)$ is the probability of an outcome $f$ conditioned on the intensity of the hazard $im$, $\left|\frac{\mathrm{d}h}{\mathrm{d}im}\right|$ is the absolute value of the derivative of the hazard curve (i.e., the slope of the hazard curve), and the integration is performed over all possible intensities of the hazard. In words, the Risk Integral is the integration of the fragility curve with the derivative of the hazard curve.

At the request of PG&E, results of the TCM are presented as annual probabilities of failure, which are calculated from $\lambda$ assuming failures follow a Poisson process:[29]

$$P(f) = 1 - e^{-\lambda}$$

where $P(f)$ is the annual probability of failure, which is the probability of at least one failure occurring in a single year.

Annual failure rate, $\lambda$, and annual probability of failure, $P(f)$, are useful measures by which assets can be risk-ranked, even for assets of different types and for different hazards. The Risk Integral provides a failure rate that reflects the underlying hazard and fragility functions. As

[29] The Poisson process assumes failures are independent with respect to time, which is a common assumption for failures associated with natural hazards.

discussed in the next section, the Risk Integral is evaluated for each component grouping subject to each applicable hazard, and the results can be combined across multiple hazards and/or multiple component groupings.

Both the fragilities and hazards might evolve with time, due to asset degradation and climate change,[30] respectively. As an example, consider the wood pole represented above in Figure 12; the pole groundline bending strength decreased by one third in 60 years due to decay. If we use the wind hazard curve shown in Figure 5, the failure rate λ can be evaluated at any time in the future to show how the failure rate is expected to increase (Figure 16). The curve is similar to the conceptual model in Figure 1.

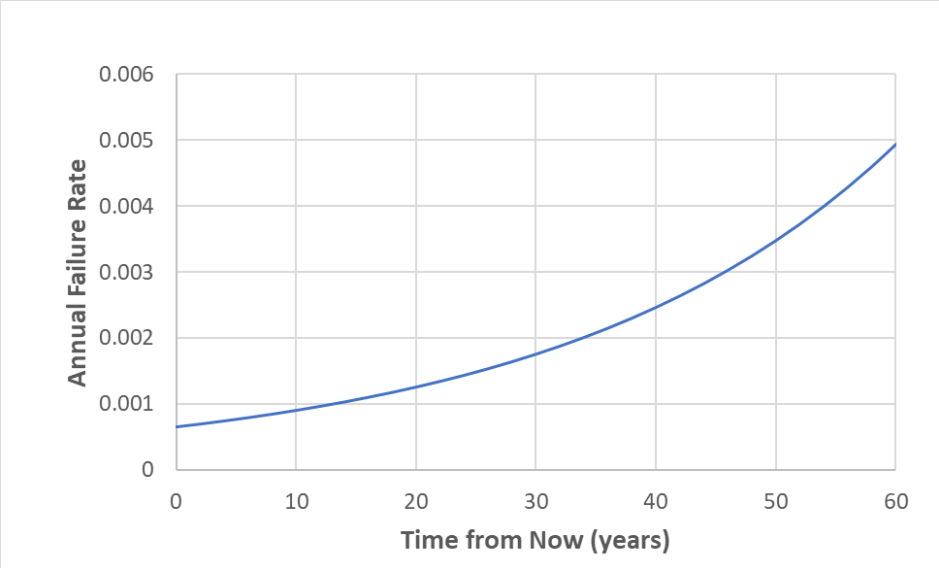


Figure 16. Increased failure rate with time for the example wood pole (Figure 12) and hazard curve (Figure 5) used for illustration in preceding sections.

The TCM currently evaluates the risk integral for five states of the fragility functions: current state, as well as forecast condition in 5, 10, 25, and 50 years. This allows users of the TCM to evaluate the increase in risk associated with an asset over time, or to predict the time at which a risk threshold will be exceeded.[31]

[30] The effect of climate change is currently outside the scope of the TCM.

[31] Future predictions of the Risk Integral assume decreased capacity continues to occur at its current rate, and increased uncertainty continues to follow the quadratic form discussed above.

# 7. Model Validation

Using available repair and outage data from PG&E, both individual threat models and annual probabilities of failure from the TCM were evaluated for their efficacy in predicting actual locations of degradation and failure among the transmission assets. The datasets used for these evaluations vary in size and content, and were generally compiled for reasons unrelated to threat model validation. Therefore, validation results presented in the following subsections are generally qualitative in nature, providing a framework by which model results can be compared to overall trends in repairs and outages. Efforts to collect additional field data for purposes of model validation are ongoing.

## Validation of Specific Threat Models

### Wood Decay Threat Model Validation

The goal of the wood decay threat model validation was to confirm that the prediction of decay progression in the TCM is consistent with decay progression measured over multiple PT&T cycles. For a total of 197 wood poles[32], the remaining strength at the date of the most recent PT&T cycle is estimated using the model described in Section 5 by extrapolation from the previous two cycles. This value is compared against the field-measured remaining strength from the third cycle, as reported in the PT&T database.

For the purpose of validation, the difference between the predicted remaining strength and the field measurement for each wood pole is calculated, and sorted into bins as presented in Figure 17. The red bars in the figure, which indicate poles with a predicted remaining strength within 10% of the field measurement, represent approximately half of the sample population (48%), showing good agreement between modeled and measured remaining strengths. Based on discussions with PG&E SMEs, the long tail of unconservative predictions (right portion of the figure) may represent poles with cross-section loss due to causes other than decay, such as

[32] Wood poles from PG&E's electric distribution network were used for the validation, since archived PT&T data for the transmission network generally did not extend far back enough to encompass three cycles. It is Exponent's understanding that poles used for the two networks are similar.

impact from vehicles or equipment. Additional studies could provide more insight on these poles; however, the wood decay model updates its predictions with each new PT&T cycle, providing means of correcting for anomalous loss of cross-section from previous cycles.

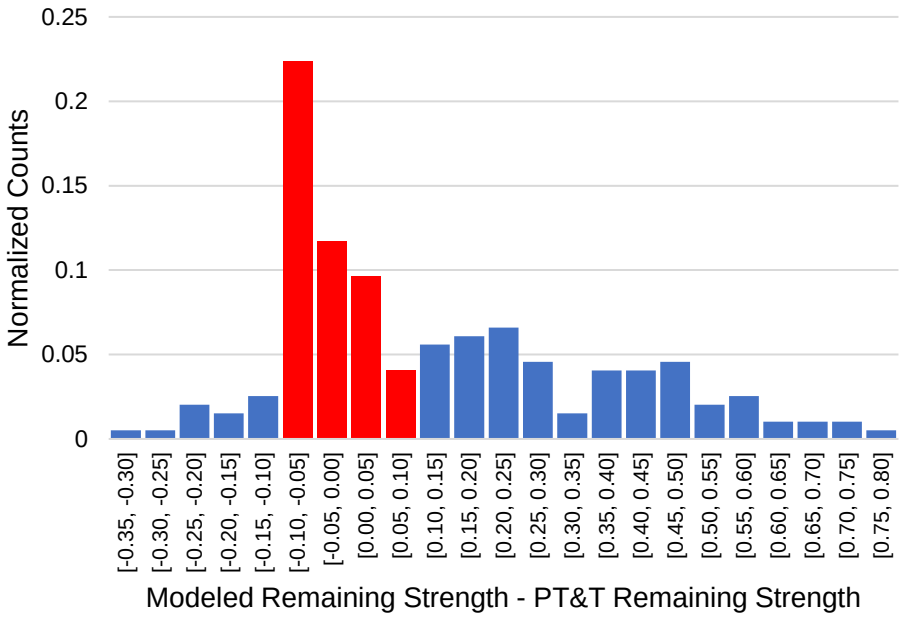


Figure 17. Normalized histogram of remaining strength difference between model prediction and field measurement.

## Atmospheric Corrosion Threat Model Validation

The goal of the atmospheric corrosion model validation was to confirm that the prediction of higher corrosion rates in the TCM are spatially correlated with incidences of corrosion-related repairs. For each asset, the corrosion category is estimated using the atmospheric corrosion model described in Section 5. Incidences of documented corrosion were obtained from repair tags, using a word search algorithm to identify corrosion and, if possible, associate it with a particular component grouping. The model is considered effective if corrosion-related repair tags occur more often in regions with higher corrosion categories predicted by the model.

Each asset has a modeled set of corrosion categories for each of four metals: carbon steel, zinc, copper, and aluminum. However, not all repair tags have an associated current SAP equipment ID number, precluding a simple matching between repair tags and corrosion category. Therefore, a nearest neighbor corrosion category map is generated that gives broader coverage over the geographic region. A 25 km x 25 km grid is created over the region, and for each grid

cell, a corrosion category is assigned based on the modeled category for the asset closest to the grid cell center. An example of this procedure is shown in Figure 18, where the individual assets, color-coded by steel corrosion category, are plotted over the nearest neighbor map. This process is repeated for each metal, for corrosion categories with and without a helical geometry factor applied (Figure 19 and Figure 20, respectively), for a total of 8 maps. The helical factor maps are used for conductor corrosion only, to account for faster corrosion rates on components with helical geometry (see memorandum in Appendix D).

Corroded components are identified through a keyword search of historical repair tags, and where possible, a combination of keyword and manual processing of this list is used to identify corrosion associated with conductors and insulators. The results are three lists of corrosion-related repair tags: (1) conductor corrosion, (2) insulator corrosion, and (3) general corrosion.

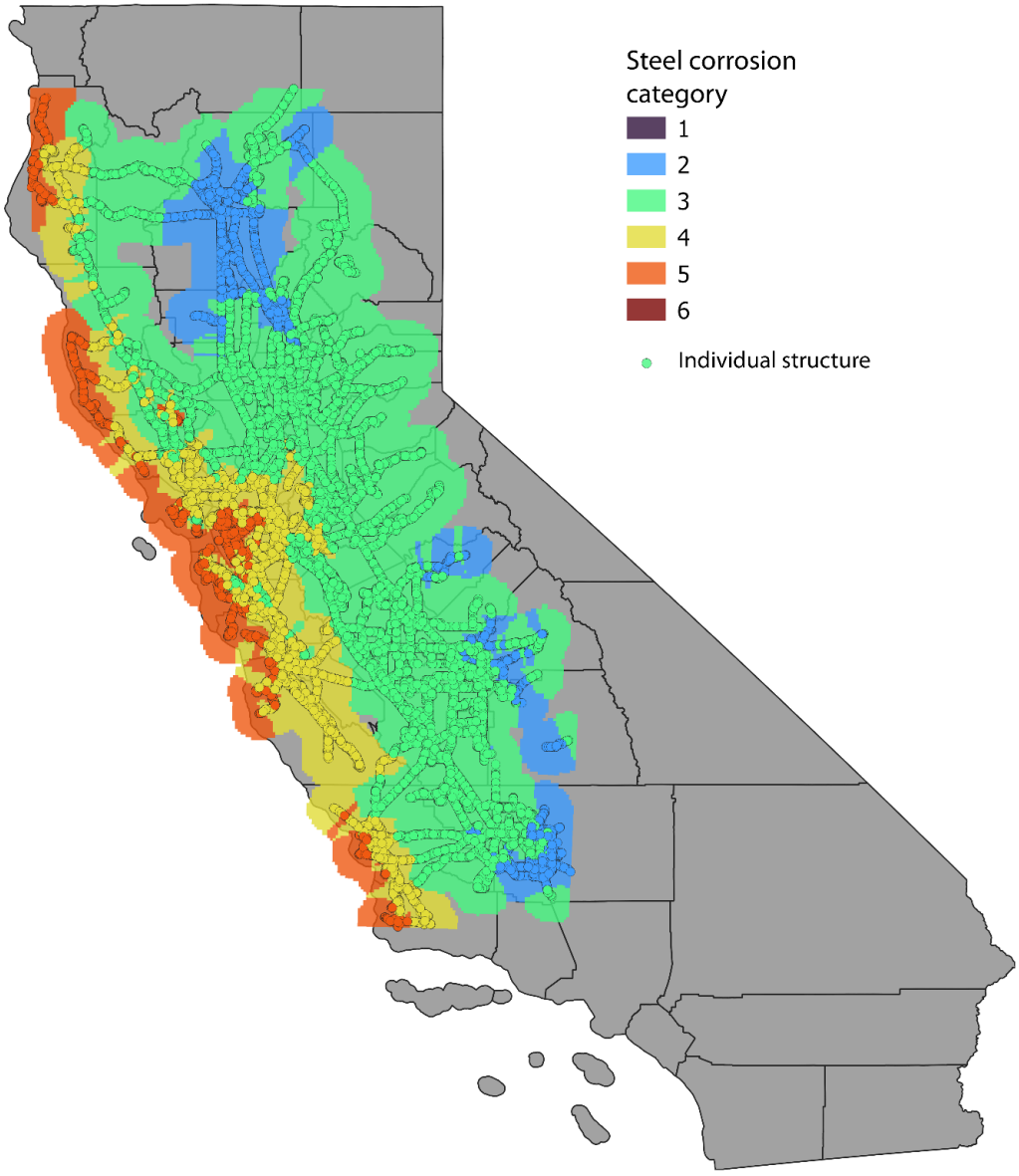


Figure 18. Nearest neighbor map generated from individual assets with assigned corrosion categories (circles).

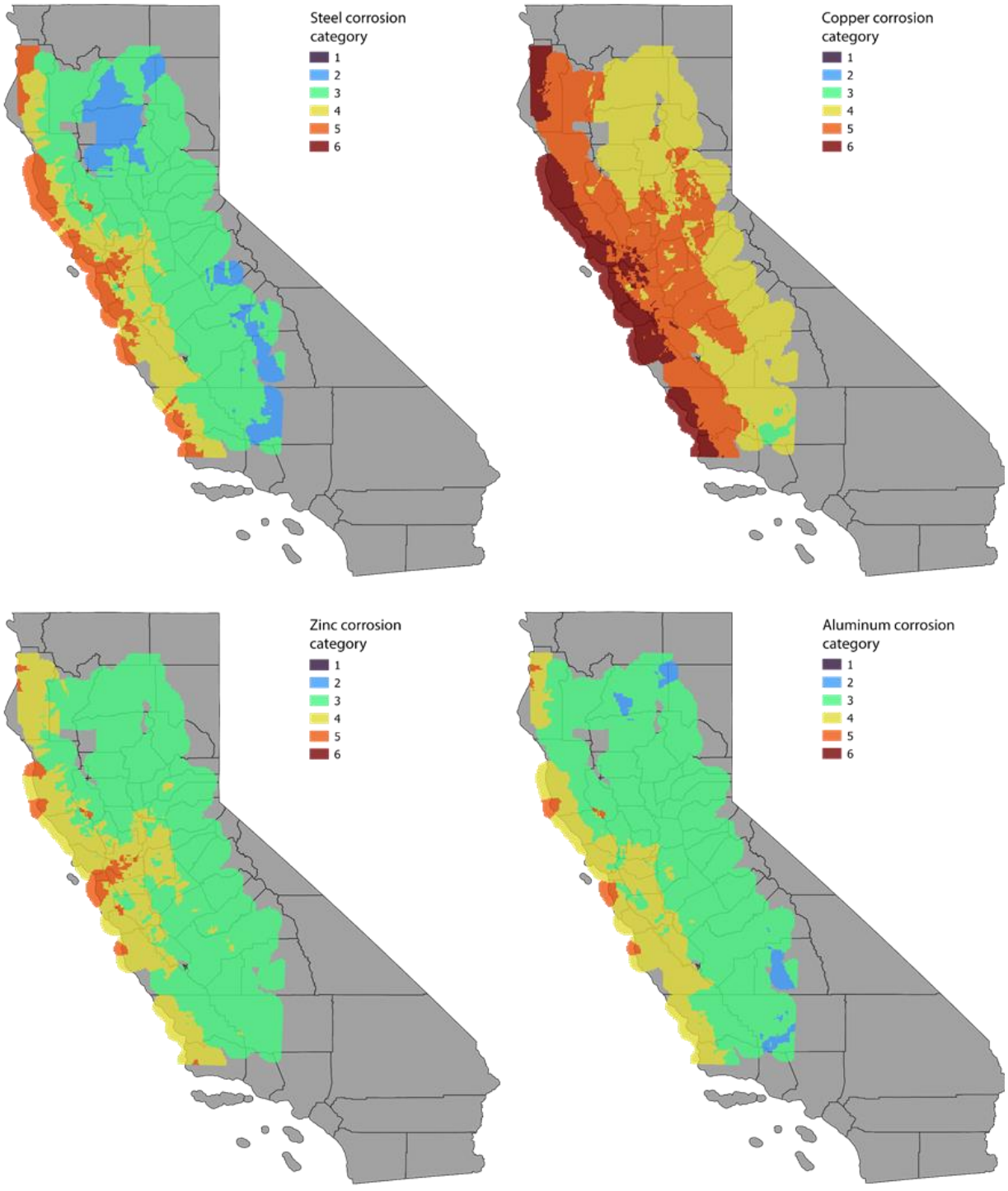


Figure 19. Corrosion category maps showing carbon steel, copper, zinc, and aluminum corrosion category for conductors.

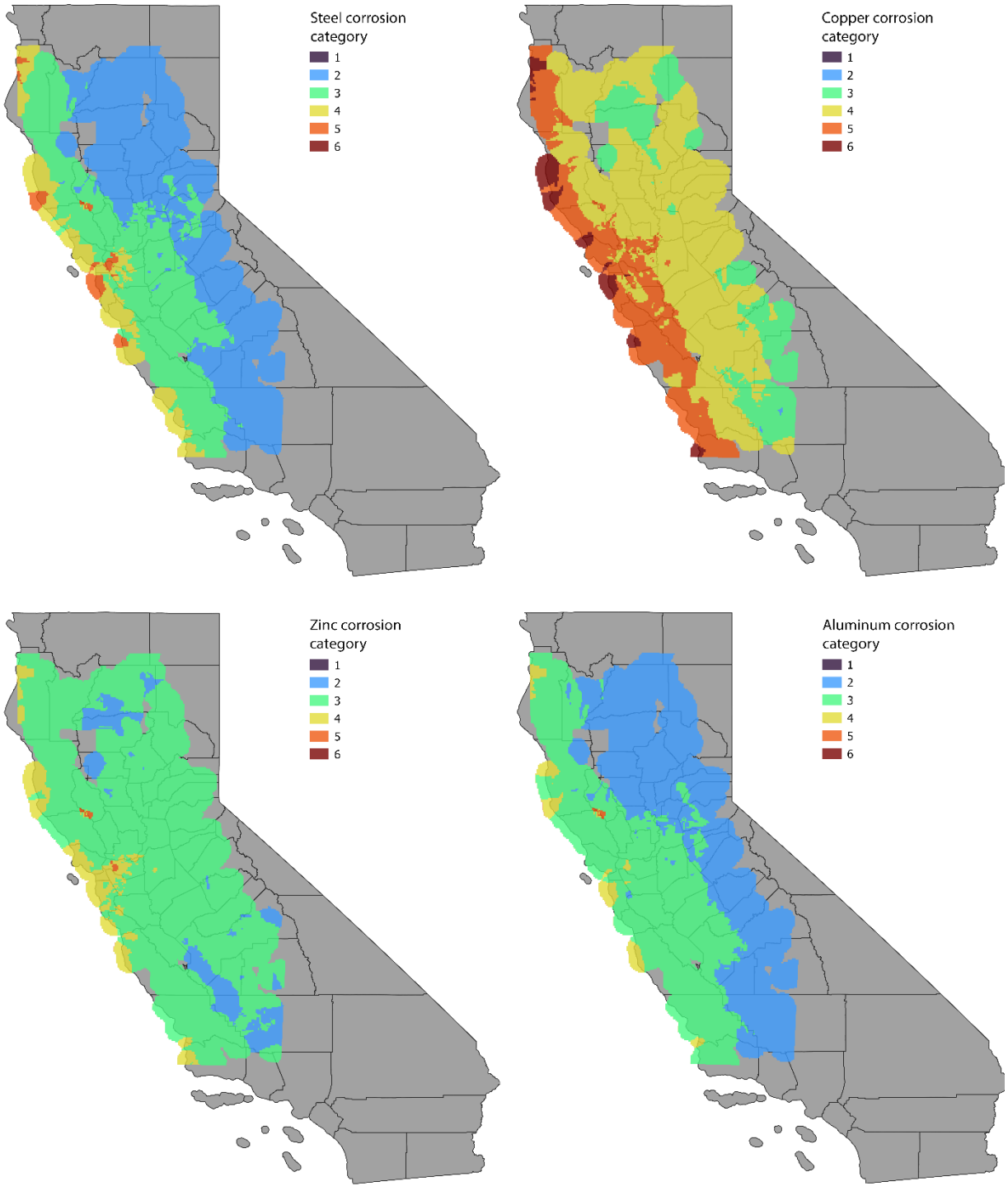


Figure 20. Corrosion category maps showing carbon steel, copper, zinc, and aluminum corrosion category for non-conductor components.

The identified repair tags are plotted geographically; a point sampling routine is used to identify the corrosion category from each corrosion category map at each repair tag location. This procedure is performed for conductors (Figure 21), insulators (Figure 22), and general components (i.e., no keyword for component grouping used) (Figure 23). Histograms of the number of tags in each corrosion category, normalized by the total fraction of assets present in each category,[33] are presented in Figure 24 through Figure 26. These normalized histograms show that, for nearly all metals and component groupings evaluated, the incidence of corrosion-related repair tags increases with more severe corrosion categories. For example, for general steel component corrosion, Figure 26 shows a steady increase in normalized repair tag counts for steel components as the corrosion category increases. In fact, the ratio of normalized repair tags in the highest modeled corrosion category compared to the lowest ranges between 6.4 and 29.7. These results suggest that the atmospheric corrosion model successfully predicts regions where higher corrosion is expected, given past corrosion-related repairs.

[33] Normalizing by the fraction of assets in a corrosion category accounts for the fact that some corrosion categories may include many more assets than others. The normalized histograms represent the relative likelihood that an asset in a given modeled corrosion category is associated with a corrosion-related repair tag.

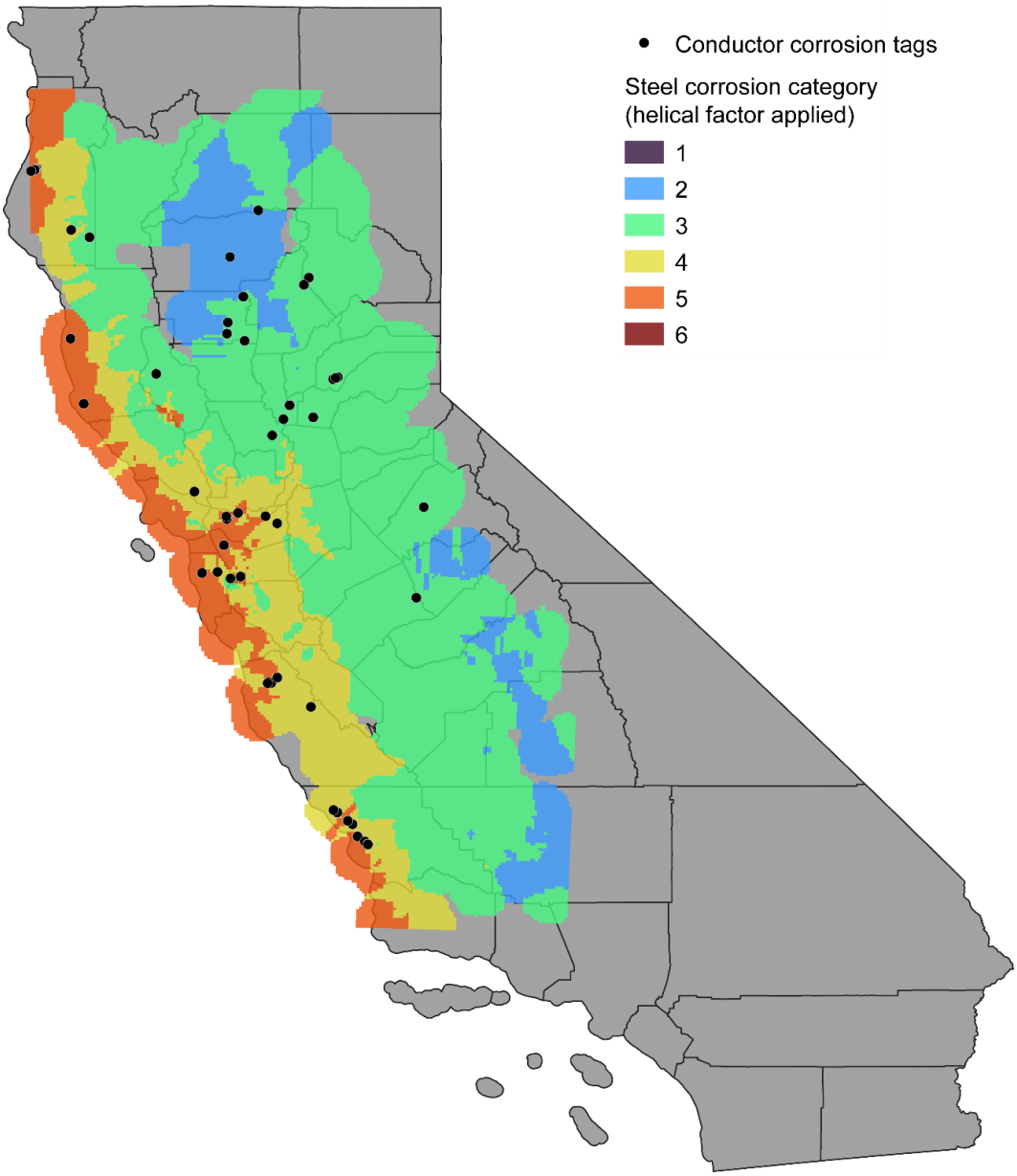


Figure 21. Conductor corrosion tags plotted over steel corrosion category.

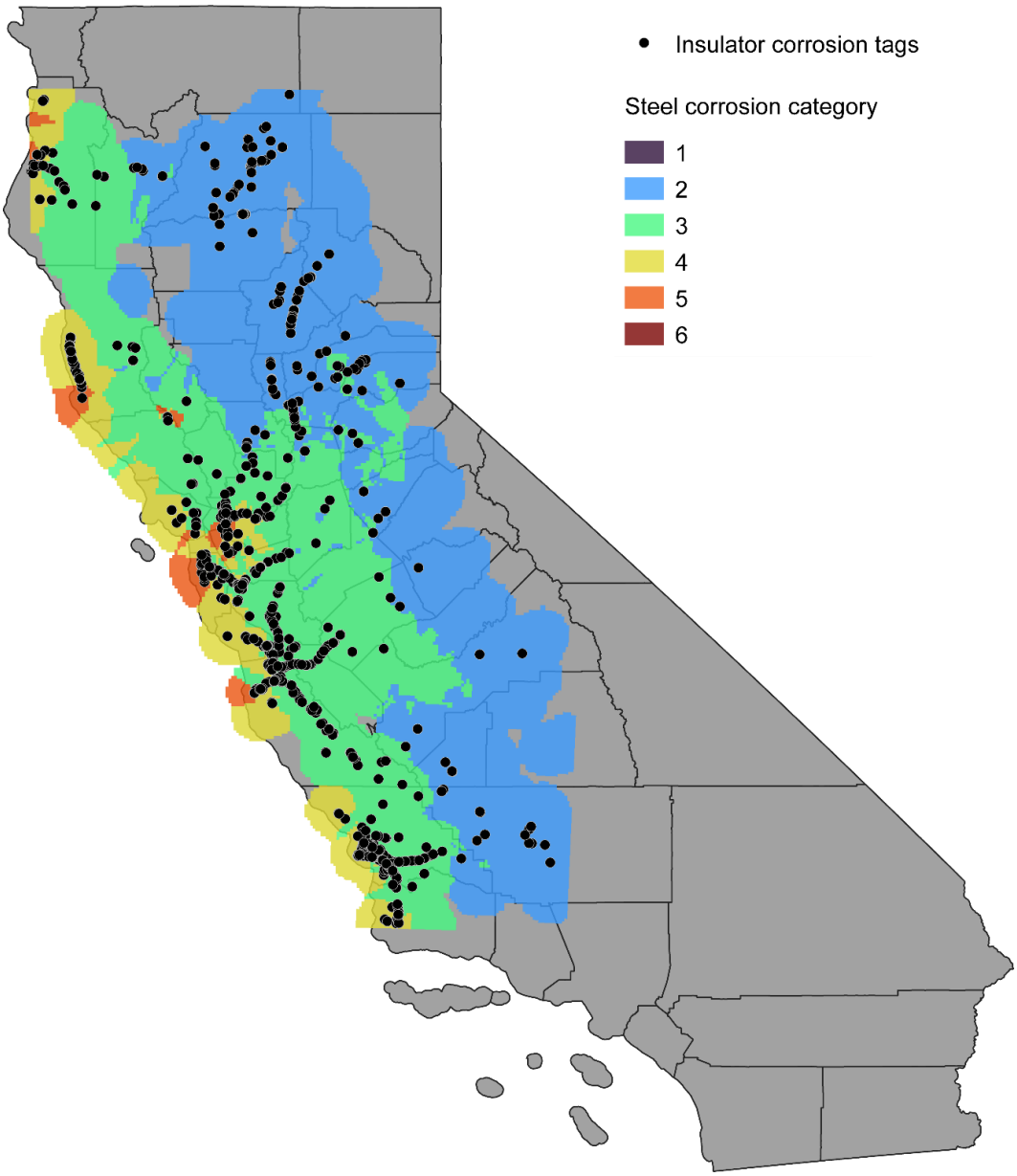


Figure 22. Insulator corrosion tags plotted over steel corrosion category.

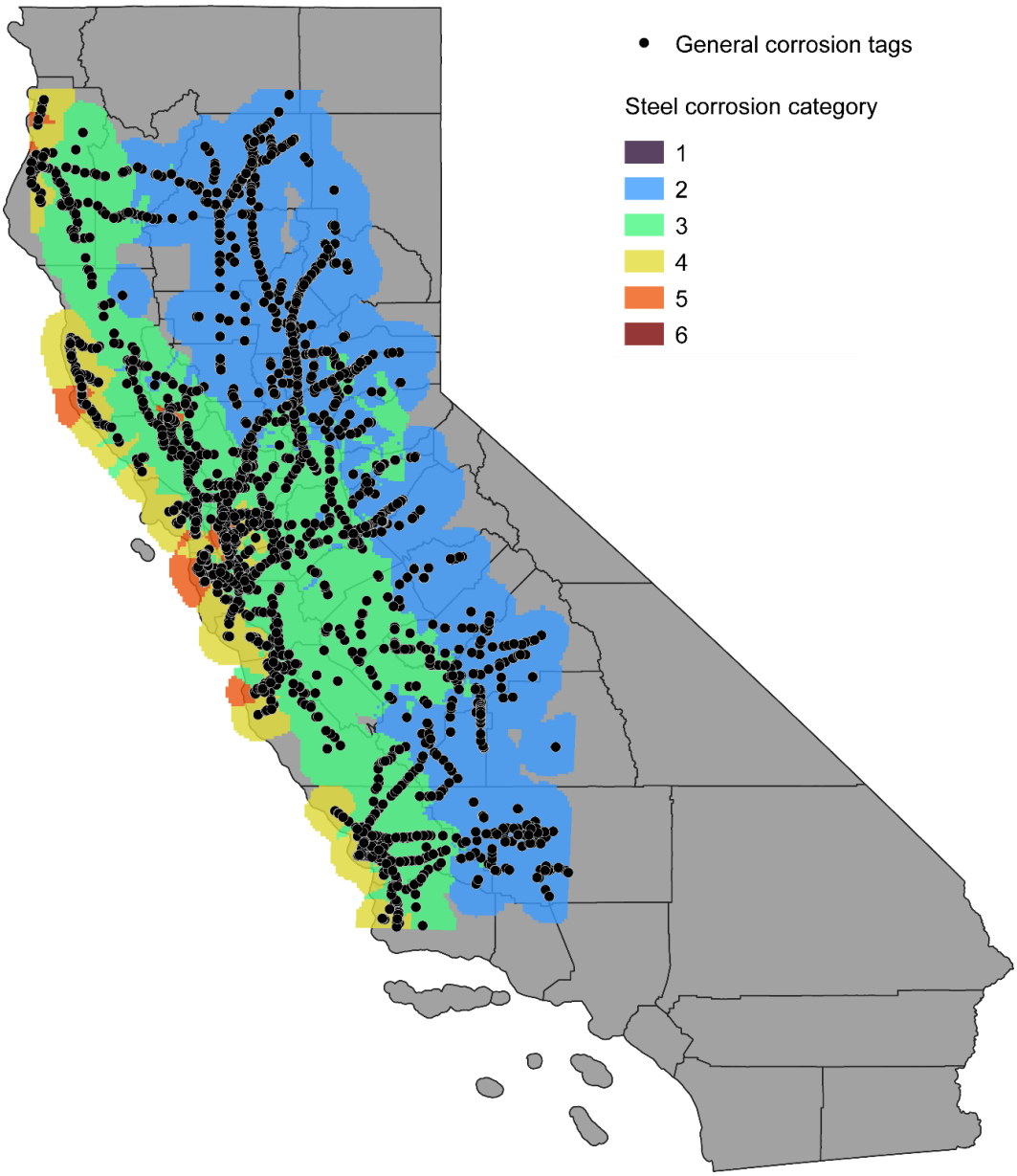


Figure 23. General corrosion tags plotted over steel corrosion category.

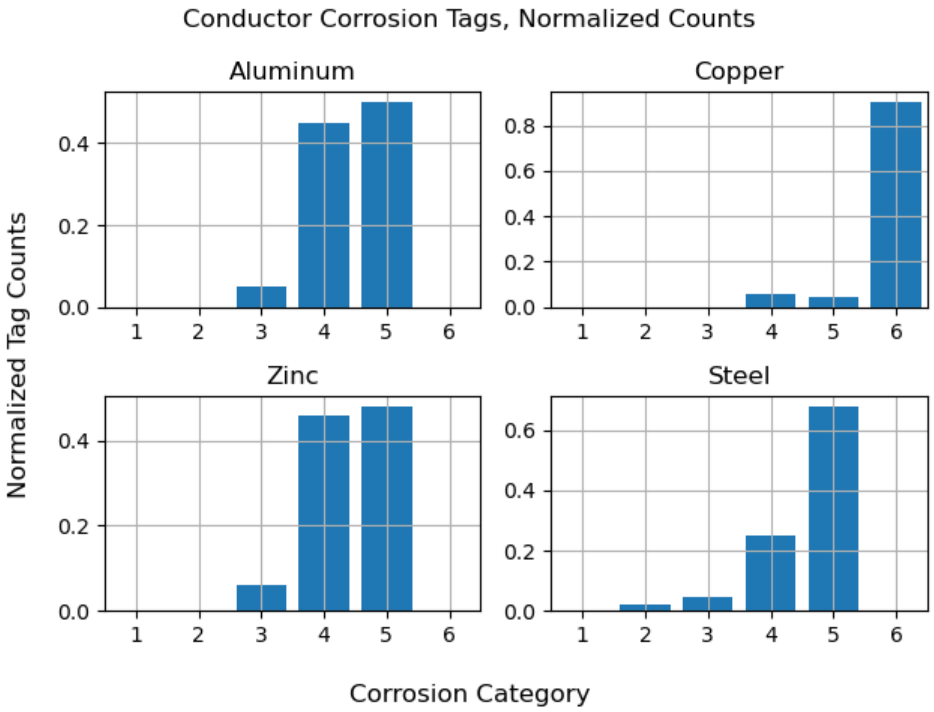


Figure 24. Normalized histograms of conductor corrosion tags per corrosion category.

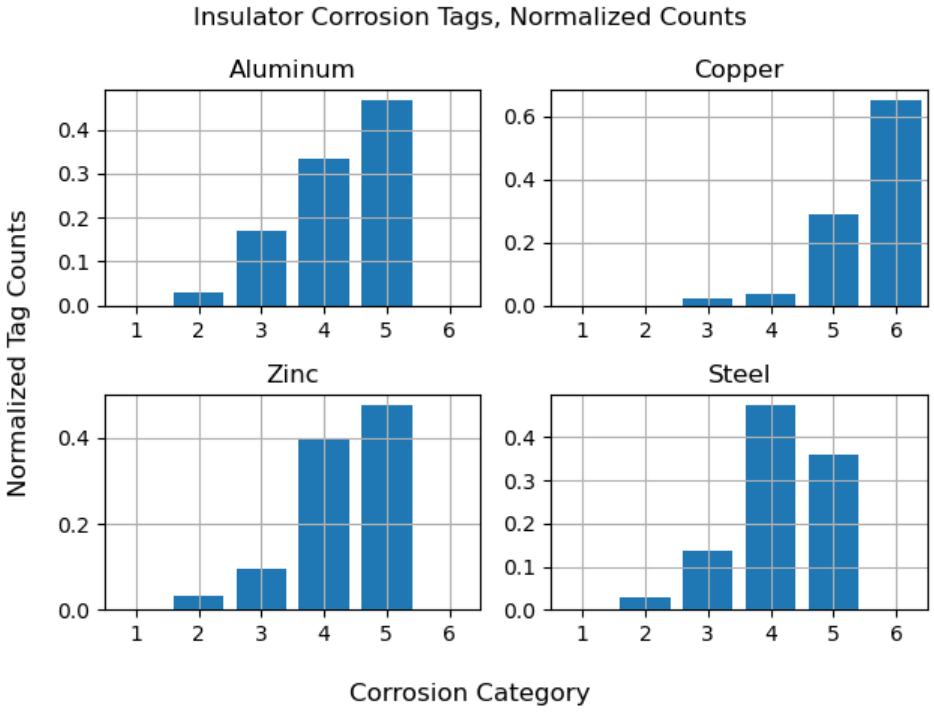


Figure 25. Normalized histograms of insulator corrosion tags per corrosion category.

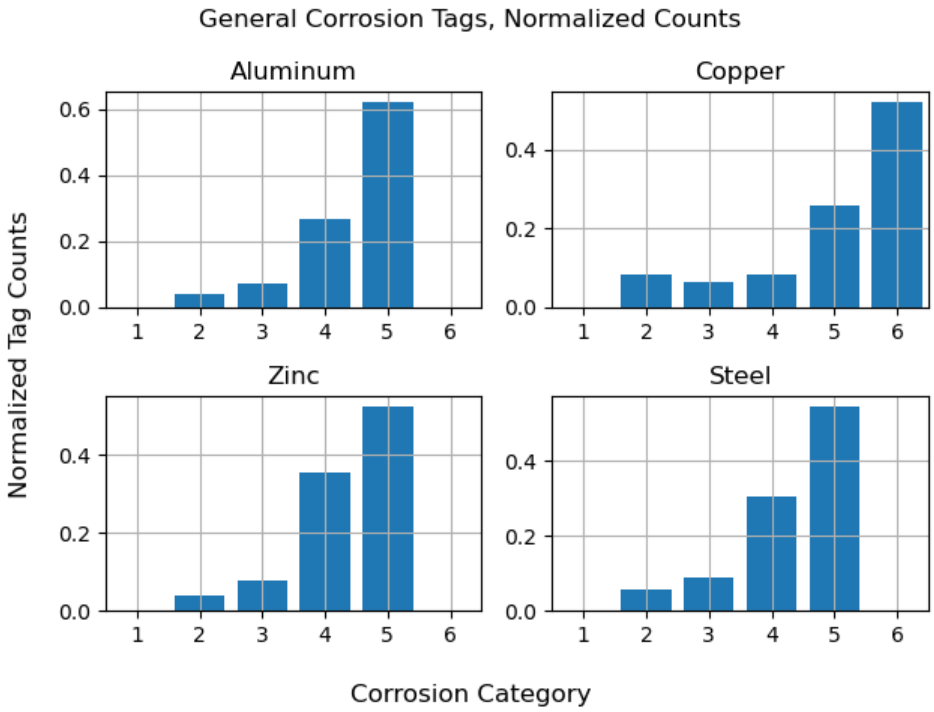


Figure 26. Normalized histograms of general corrosion tags per corrosion category.

## Underground Corrosion Threat Model Validation

The goal of the underground corrosion threat model validation was to confirm that predictions of higher corrosion rates in the TCM are spatially correlated with field observations of corrosion on buried tower legs. For the purpose of validation, field inspections of 610 tower legs were compared with predicted corrosion potential (high, moderate, and low) using the underground corrosion model described in Section 5. The model is considered effective if tower legs with high and moderate modeled corrosion categories correlate with field observations of corrosion.

Based on the field inspection results, 596 of 610 buried tower legs exhibited corrosion, and the other 14 did not. These results are presented for each modeled corrosion category in Figure 27. The results show that corrosion was observed in the field for 98% of tower legs with modeled high or moderate corrosion potential, suggesting good correlation between model prediction and field observation for these two categories.

However, only six tower legs with corrosion observed in the field have modeled corrosion potential of low, which is considered too small of a sample set to draw meaningful conclusions

regarding this corrosion category. Additional studies could provide more insight into the predictive capabilities of the model for assets in areas of low modeled corrosion potential.

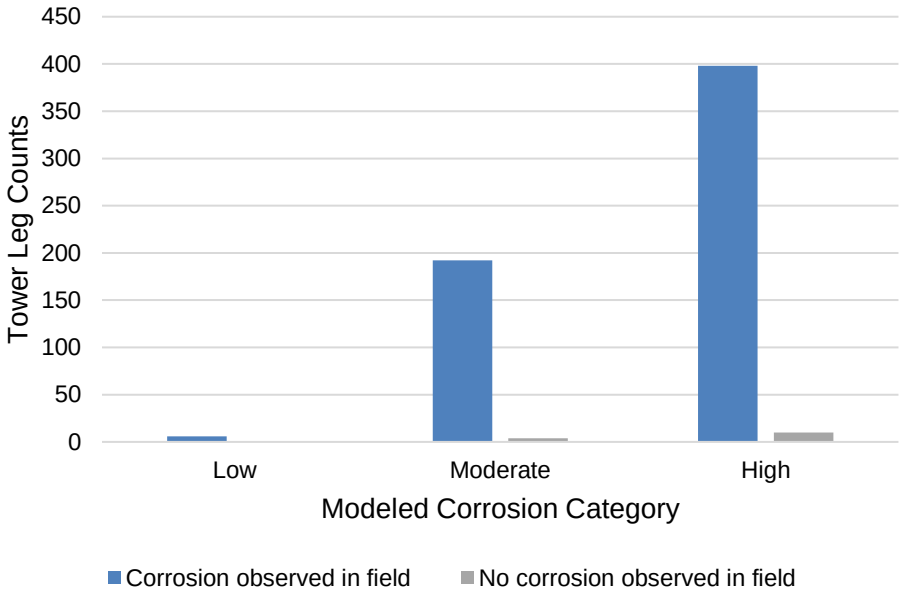


Figure 27. Histogram of tower leg corrosion field observations.

## Fatigue Threat Model Validation

The goal of the fatigue threat model validation was to confirm that predictions of higher susceptibility to aeolian vibrations in the TCM are spatially correlated with incidences of damper-related repairs.[34] For each conductor, the aeolian vibration DLRF is estimated using the fatigue model described in Section 5. Incidences of damper-related repairs were obtained from damper repair tags and, if possible, associated with an individual asset by SAP equipment ID. The model is considered effective if damper-related repair tags occur more frequently on assets with conductors having higher aeolian vibration DLRFs.

As discussed in Appendix F, depending on susceptibility to aeolian vibrations, each conductor is assigned an aeolian vibration DLRF of 0, 0.1, 0.2, and 0.333. A normalized[35] histogram of damper-related repair tags by each DLRF category is presented in Figure 28, which shows a

[34] Fatigue-related damage is very difficult to observe in the field, so damage to dampers was used as a surrogate.

[35] Normalizing by the fraction of assets accounts for the fact that some DLRF categories may include many more assets than others. The normalized histograms represent the relative likelihood that a conductor in a given modeled DLRF category is associated with a damper-related repair tag.

steady increase in normalized repair tag counts as DLRF increases. In fact, the ratio of normalized repair tags in the highest modeled aeolian vibration DLRF category compared to the lowest is approximately 7.5. This suggests that the fatigue model successfully predicts conductors that are more prone to aeolian vibrations.

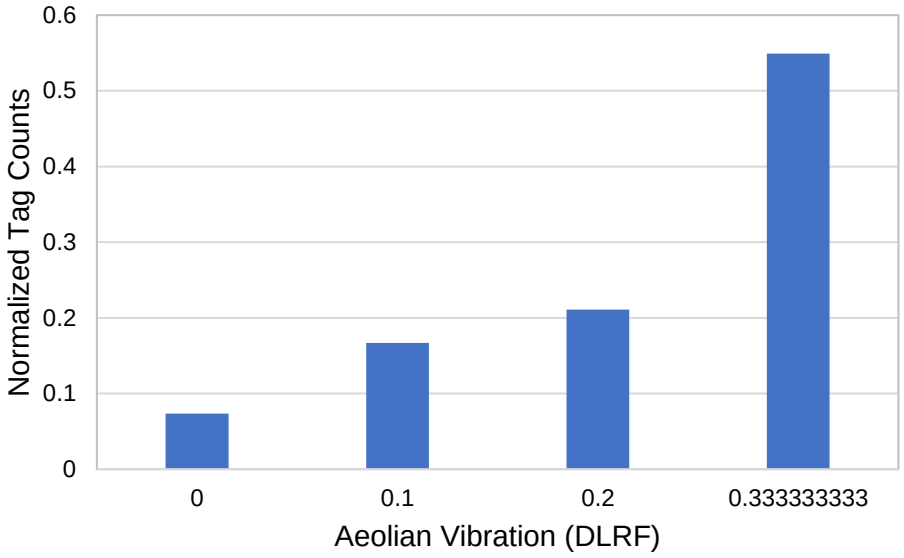


Figure 28. Normalized histogram of damper-related repair tags per DLRF.

## Mechanical Wear Threat Model Validation

As discussed in Section 5, the results of Exponent's first-principles wear model is used as an input parameter for a machine learning model by PG&E. Validation of this model is performed separately.[36]

## Polymer Insulator Aging Threat Model Validation

The goal of the polymer insulator aging threat model validation was to confirm that the mechanical degradation predictions by the TCM are spatially correlated with incidences of polymer insulator replacements. Incidences of polymer insulator replacements were obtained from the available insulator replacement tags with keywords suggesting the presence of a

[36] "Transmission Line: Above Grade Cold-end Hardware Mechanical Wear Model, Version 2 (MechWear-v2)," June 2023, by Sasha Yan (PG&E).

polymer insulator at the tag location.[37] The polymer insulator aging model described in Section 5 is used to estimate the DLRF at the location of each replacement tag. The model is considered effective if polymer insulator replacement tags occur more frequently at locations having higher polymer insulator aging DLRFs.

The locations of 1,642 polymer insulator replacement tags were available. The DLRFs predicted by the model at the tag locations ranged between 0.47 and 0.74, where higher DLRF indicates higher susceptibility to mechanical degradation, as discussed in Appendix I. A normalized histogram of polymer insulator replacement tag counts corresponding to different DLRFs is presented in Figure 29, where each histogram bar represents a range of DLRF values between 0.4 and 0.8. The figure shows a substantial increase in the replacement tag density (normalized counts)[38] as the DLRF increases, especially for insulators with DLRFs larger than 0.5. The ratio of the replacement tag density in the bin with the highest DLRF values (ranging between 0.7 – 0.8) to the bin with the lowest DLRF values (ranging between 0.4 and 0.5) is approximately 8.2. This observation suggests that the polymer insulator aging model successfully predicts the locations of polymer insulators with higher vulnerability to degradation, as reflected by the larger number of replacement tags.

[37] The polymer insulator replacement tags are not exclusively indicative of mechanical failure, and some may indicate electrical failures. However, the environmental factors contributing to the high vulnerability to electrical failures are considered relevant for mechanical degradation and strongly influence the polymer degradation model predictions.

[38] Normalizing by the fraction of assets accounts for the fact that some DLRF categories may include many more assets than others. The normalized histograms represent the relative likelihood that an asset in a given modeled DLRF bin is associated with a polymer insulator replacement tag.

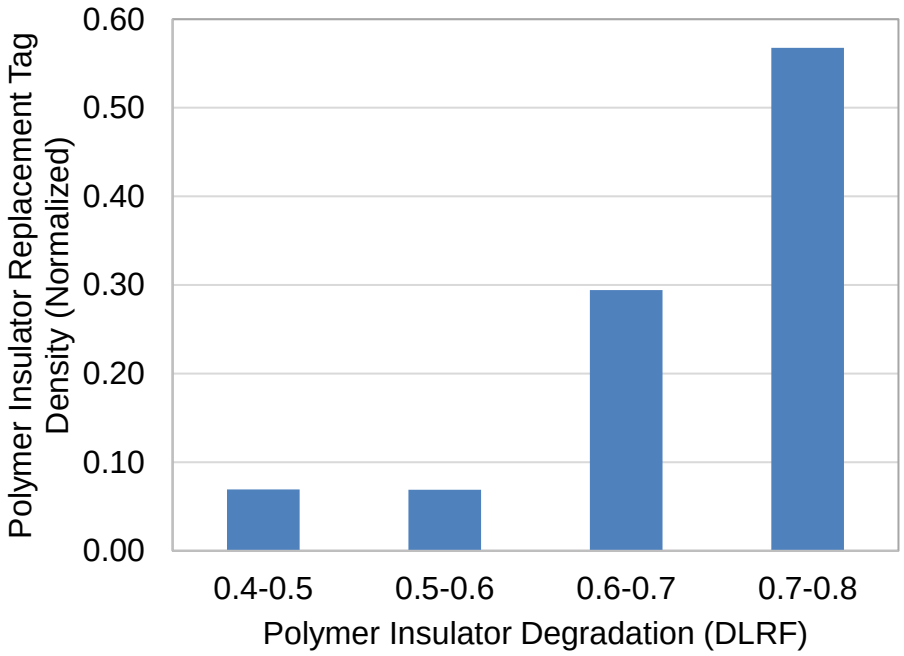


Figure 29. Normalized histogram of polymer insulator replacement tags binned by predicted DLRFs.

## Validation with Outages

### Wind Annual Probability of Failure Validation

The goal of the wind annual probability of failure validation was to confirm that predictions of higher annual probabilities of failure in the TCM wind model are correlated with wind-related outages. For each asset, the probability of failure caused by wind is calculated using the "multi-feature" mode of the TCM wind model described in Section 4. Incidences of wind-related outages were obtained from PG&E's outage history database and, if possible, associated with an individual asset's probability of failure by concatenating the ETL number with the structure number.[39] The model is considered effective if wind-related outages occur more frequently on assets with higher probabilities of failure due to wind.

For the purpose of the validation, wind-related outages from the database were binned using the 50$^{th}$ (median), 60$^{th}$, 70$^{th}$, 80$^{th}$, and 90$^{th}$ percentile values of the estimated probabilities of failure from the TCM wind model for all assets as presented in the histogram of Figure 30. The results

[39] Not all outages in the database are associated with a particular asset or location.

are compared to the expected distribution if wind-related outages were "random" or uncorrelated with probability of failure estimated by the model (black dashed line in figure). The results show clear correlation; for example, about 91% and 39% of the wind-related outages occurred on assets with predicted probability of failure higher than the median value and the 90$^{th}$ percentile value, respectively. For the random case, 50% and 10% would have been expected, respectively. This correlation was anticipated, given the statistical (Bayesian inference) model used to adjust the asset fragility functions based on past wind outages, as discussed in Section 4.

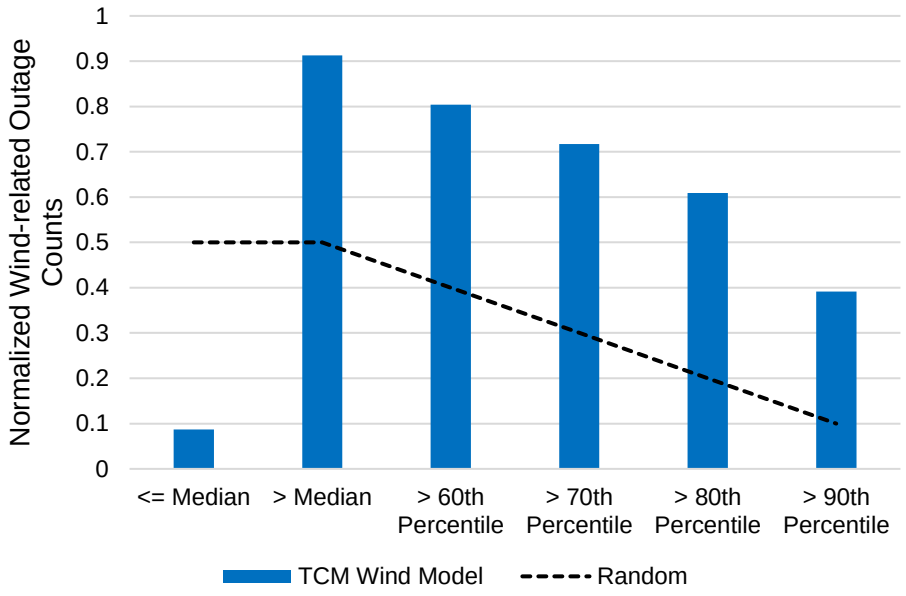


Figure 30. Normalized histogram of wind-related outages per probability of failure percentile bin.

## Insulator Contamination-Induced Flashover Annual Probability of Failure Validation

The goal of the insulator contamination model validation was to confirm that predictions of higher probabilities of flashover in the TCM are correlated with contamination-related outages (non-animal-caused). For each asset, the probability of flashover caused by insulator contamination is calculated using the insulator contamination model described in Section 5. Incidences of contamination-related outages were obtained from PG&E's outage history database and, if possible, associated with an individual asset's probability of flashover by

concatenating the ETL number with the structure number.[40] The model is considered effective if contamination-related outages occur more frequently on assets with higher probabilities of flashover.

For the purpose of validation, contamination-related outages from the database were binned using the 50th (median), 60th, 70th, 80th, and 90th percentile values of the estimated probabilities of flashover from the TCM model for all assets as presented in the histogram of Figure 31. The results are compared to the expected distribution if contamination-related outages were "random" or uncorrelated with probability of flashover estimated by the model (black dashed line in figure). The results of the current model do not show good correlation; for example, approximately 65% of the outages occurred on assets with predicted probability of flashover less than the median value. As discussed in Section 5, work on the insulator contamination model is ongoing.

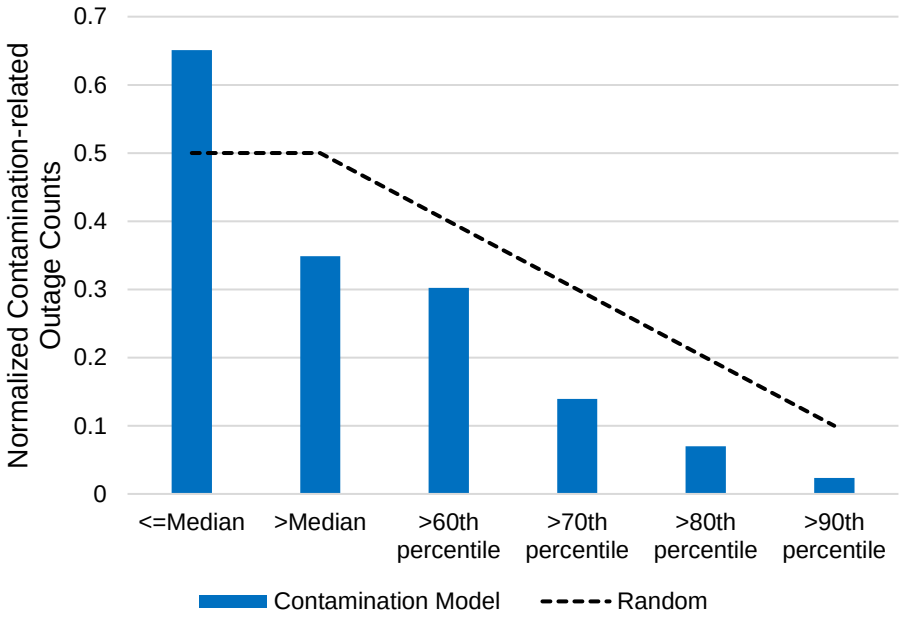


Figure 31. Normalized histogram of contamination-related outages per probability of flashover percentile bin.

[40] Not all outages in the database are associated with a particular asset or location.

# 8. Combining Annual Probabilities of Failure

The annual probabilities of failure described in the preceding section are combined in the TCM in three primary ways:

1. For a single hazard (e.g., wind), annual probabilities of failure for all component groupings of an asset are combined. The resulting probability of failure represents the annual likelihood that at least one component grouping of the asset will fail due to the hazard of interest. This is referred to herein as the *single hazard, asset-level, annual probability of failure.*
2. For all hazards, annual probabilities of failure for a single component grouping of an asset (e.g., conductor) are combined. The resulting probability of failure represents the annual likelihood that the component grouping will fail due to at least one hazard. This is referred to herein as the *multi-hazard, component grouping-level, annual probability of failure*.
3. For all hazards, annual probabilities of failure for all component groupings of an asset are combined. The resulting probability of failure represents the annual likelihood that at least one component grouping of the asset will fail due to at least one hazard. This is referred to herein as the *multi-hazard, asset-level, annual probability of failure.*

The procedures used to combine annual probabilities of failure for these three cases are described below.

## Single Hazard, Asset-Level, Annual Probability of Failure

For a single hazard, the asset-level annual probability of failure can be computed in several ways, based on assumptions regarding the correlation between component groupings. For the uncorrelated (mutually independent) case, the annual probability of failure is computed based on the product of the survival rates for each component grouping subject to the hazard of interest:

$$P(f)_{single\ hazard,asset,uncorrelated} = 1 - \prod_{i=1}^{m}(1 - P(f)_{single\ hazard,component\ grouping_i})$$

where *m* is the total number of component groupings. The uncorrelated case represents the upper bound annual probability of failure.

For the assumption of fully correlated component groupings, the annual probability of failure is equal to the maximum of the annual probabilities of failure for all component groupings:

$$P(f)_{single\ hazard,asset,fully\ correlated} = maximum(P(f)_{single\ hazard,component\ grouping_{i=1\ldots m}})$$

The uncorrelated case represents the lower bound annual probability of failure. Since we currently have no information on which of the upper or lower bound assumptions is more correct in any given circumstance, we average the two bounds:

$$P(f)_{single\ hazard,asset} = average(P(f)_{single\ hazard,asset,uncorrelated}, P(f)_{single\ hazard,asset,fully\ correlated})$$

## Multi-Hazard, Component Grouping-Level, Annual Probability of Failure

Because hazards considered to date by the TCM are assumed to be uncorrelated (e.g., wind and earthquake loading are mutually independent), annual failure rates for different hazards can be added within a component grouping:

$$l_{multi\ hazard,component\ grouping} = \sum_{j=1}^{n} l_{single\ hazard_j,component\ grouping}$$

where *n* is the total number of independent hazards. The multi-hazard, component grouping-level annual probability of failure is then computed as:

$$P(f)_{multi\ hazard,component\ grouping} = 1 - e^{-l_{multi\ hazard,component\ grouping}}$$

## Multi-Hazard, Asset-Level, Annual Probability of Failure

Again, because hazards considered to date by the TCM are assumed to be uncorrelated, the multi-hazard, asset-level, annual probability of failure is computed based on the product of the survival rates for each single hazard, asset-level annual probability of failure:

$$P(f)_{multi\ hazard,asset} = 1 - \prod_{j=1}^{n}(1 - P(f)_{single\ hazard_j,asset})$$

# 9. Statistical Assessment of Transmission Line Performance Under Wind Loads

## Background

The Bayesian Update (BU) model represents the probability of transmission structures experiencing a failure under various wind loads. The BU model is statistical in nature and relates the probability of a failure (transmission outage) to a particular wind load (maximum daily 3-second gust velocity).

From 2020 to 2022, the probability of an outage at a particular structure on a particular day was modeled as a function of wind speed:

$$P(outage) = \Phi\left(\frac{\ln v - \mu}{\beta}\right)$$

where $v$ is the maximum daily wind speed and $\mu$ and $\beta$ are parameters shared by all structures for a particular transmission line. This corresponds to a probit regression model for the probability of an outage. Note that this is a Bayesian model, and full details on the model specification and fitting procedures may be found in the document titled *A Framework for Risk-Based Transmission Line Asset Management and Operability Assessment, Revision 7*, by Exponent, dated January 13, 2023.

From 2020 to 2022, the BU model was fit using "vetted wind outages", which were transmission outages that were labeled as wind-related by a PG&E SME . There were known challenges associated with the use of these labeled outages, including "wind-related" outages at unrealistically low wind speeds. These were likely mislabeled as wind-related, and they could exert a high degree of influence on the BU regression model. In addition, other categories of outage, such as equipment failure, exhibited disproportionately high rates at high wind speeds, suggesting that some true wind-related outages were being missed.

The BU model has certain limitations linked to the availability of training data. The model treats all structures on a particular transmission line, or circuit, as having an equal conditional probability of failure for a given windspeed. This is due to the fact that outages are reported at the line level, and there may not be a specific known structure associated with the outage.

# 2023 Updates

## Overview

The BU model was modified in 2023 to improve its robustness to mislabeled wind outages and to allow it to use a higher proportion of available outage data. This updated model was used for both Operational Assessment (OA) and TCM applications beginning in the summer of 2023.

## Model Update: Extension to Allow for Non-Wind-Caused Outages

The 2020 to 2022 BU model was fit under the assumption that all outages used for model fitting were caused by wind loading on structures. This model was fit using only SME labeled wind-caused outages, as determined by PG&E, and therefore did not use information from the vast majority of recorded outages.

As noted previously, this version of the BU model was sensitive to mislabeling in the vetted wind outage dataset. For example, when low-wind outages were inaccurately labeled as caused by wind, the model would make excessively conservative adjustments to the fragility of structures on the corresponding transmission line.

The 2023 update to the BU model modified the probability of an outage to account for non-wind-caused outages:

$$P(outage) = \alpha + (1 - \alpha)\Phi\left(\frac{\ln v - \mu}{\beta}\right).$$

Here, $\alpha$ is a new parameter representing the wind-independent probability of an outage. The parameter $\alpha$ is learned along with $\mu$ and $\beta$ in the model-fitting process.

Intuitively, this updated model allows each structure to have a baseline non-wind-dependent failure rate $\alpha$ in addition to the original wind-dependent failure rate $\Phi\left(\frac{\ln v - \mu}{\beta}\right)$. This makes the model much more robust to low-wind-speed outages, which are now primarily attributed to the baseline failure rate. The model is still Bayesian, and the prior for $\alpha$ is a uniform distribution on the interval from 0 to 1.

This model can be used to perform *soft classification* for outages, which provides a probability that a given outage is wind related based on the values of $\mu$ and $\beta$ for the line and the wind

speed at the time of the outage. This is done by dividing the probability of an outage attributable to wind by the overall probability of an outage:

$$P(wind\ related\ outage|outage, v) = \frac{P(wind\ related\ outage|v)}{P(outage|v)}$$

$$= \frac{\Phi\left(\frac{\ln v - \mu}{\beta}\right)}{\alpha + (1-\alpha)\Phi\left(\frac{\ln v - \mu}{\beta}\right)}.$$

### Data Update: Use of Additional Outage Data

Prior to this update, the BU model was trained on a vetted wind outages dataset, which included a subset of outages manually selected to likely have been caused by wind loading on structures. This dataset contained 355 outages through 2022.

The model update described above enables the BU model to include both wind-caused and non-wind-caused outages. To train this model, the outage dataset is expanded to include all outages with labeled cause categories in: Weather, Equipment Failure, and Unknown. The expanded outage dataset includes 8,657 outages through 2022. By including the expanded outage dataset, the BU model can now capture information from wind-related outages that had previously been attributed to a different cause.

### Software Implementation

As part of the transition to the new model, the Bayesian Update computer code was rewritten in STAN, as opposed to the prior implementation in BUGS. This change did not have any noticeable impact on model results.

## 2024 Updates

### Overview

The 2024 update changes the BU model to separately estimate failure probabilities for each of eight specific component groupings. This version of the BU model was used for TCM modeling starting in fall of 2024, but it is not currently used for OA applications.

## Model Update: Sperate Outage Models for Component Groupings

Prior to this update, the BU model was trained on all outages related to a given subset of potential causes. As a result, the BU model estimated the probabilities that *any* component on an ETL would fail.

In the TCM settings, however, it is useful to estimate failure probabilities for specific component groupings. For example, a stakeholder responsible for wood poles may want to know the probability that a wood pole on a given ETL will fail in the next year, rather than the overall probability of any component failure on the ETL.

To target the BU model at specific component groupings, separate BU models are fit for each component grouping. This results in eight BU models, for the eight component groupings: **conductors, insulators, non-steel structures, steel structures, foundations, above grade hardware (AGH), below grade hardware (BGH), and splices**. Component grouping classes are based on standardized internal classifications as discussed above.

Each component-grouping model is fit on a different subset of labeled outages (i.e., failures), and uses a different component count to determine exposure to potential failures. The procedures for producing the component-grouping specific outages and component counts are outlined in the following sections.

The outages used by each component-grouping BU model are determined via a two-stage process. First, each outage is assigned a label based on data recorded about the Family and T-Line Asset that failed, as illustrated in Table 2.

Table 2. Logic for attributing outages to specific component groupings

| What_Family_Failed | What_T_Line_Asset_Failed | Component grouping label |
|---|---|---|
| Conductor | Detected splice keywords: splice, sleeve | **Splice** |
| | No detected splice keywords | **Conductor** |
| Insulator | All | **Insulator** |
| Hardware | Detected BGH keywords: anchor | **BGH** |
| | No detected BGH keywords | **AGH** |
| Non-Steel Structures | All | **Non-steel structure** |
| Pole | | |
| Structure | | |
| Steel Structures | Detected foundation keywords: foundation, concrete, rebar, footing, encased, encasing, stub | **Foundation** |
| | No detected foundation keywords | **Steel structure** |
| Unknown | All | **Unknown** |
| None | | |

Then, outage datasets for each component-grouping BU model are constructed. The dataset for each component grouping is constructed *conservatively*, i.e., any outage that could have been caused by a given component grouping is included in the outage dataset for the BU model for the component grouping. This ensures that the new component-grouping BU model will not undercount labeled failures for any component grouping. Table 3 demonstrates the outages included in the outage datasets for each component-grouping BU model.

Note that there is a distinction between outages that do not have a label for which component grouping contributed to the outage versus outages for which the label is "Unknown". As discussed previously, not all outages are attributed to specific structures on a transmission line, and consequently the more detailed information about what component grouping on a structure contributed to the outage is also unavailable. However, in some cases this information is missing because PG&E's internal processes for assessing the outage are not complete. In such cases, the component grouping label is currently missing, but may become known at some point in the future. However, since there is currently no information about the outage, it is not currently possible to rule out any component grouping as being the cause.

In other cases, an outage has been investigated, but the component grouping causing the outage was still not identified. In these cases, the component grouping label will be "Unknown". This may happen when the cause of the outage was transient and therefore not identifiable upon subsequent inspection. In such cases, no additional information regarding the outage cause will ever be known, but certain causes can be ruled out due to the lack of physical evidence. For example, if an outage is caused by a wood pole failure, the failed pole would still be evident after the outage. Therefore, while an outage with a missing label may have been caused by a wood pole, an outage with an "Unknown" label could not have been.

Table 3. Logic for labeling outages based on labeled component groupings responsible for the outage

| Conservative outage label | Outage component grouping labels included |
|---|---|
| **Splice** | Missing label, labeled “Splice”, labeled “Unknown” |
| **Conductor** | Missing label, labeled “Conductor”, labeled “Unknown” |
| **Insulator** | Missing label, labeled “Insulator”, labeled “Unknown” |
| **BGH** | Missing label, labeled “BGH” |
| **AGH** | Missing label, labeled “AGH”, labeled “Unknown” |
| **Non-Steel Structure** | Missing label, labeled “Wood pole” |
| **Foundation** | Missing label, labeled “Foundation” |
| **Steel Structure** | Missing label, labeled “Steel Structure” |

Note that as of the last time the BU model was run, May 2024, over two-thirds of the outages between 2007-2022 that are used by the BU model are missing component grouping information. Additionally, the data used in the May 2024 model run contained zero labeled BGH outages. The resulting estimates from the BGH model, which attributed all outages with missing component groupings to the subset of structures with BGH, produced failure rate estimates that did not appropriately reflect the low rate of labeled BGH outages. At the same time, it would have been inappropriate to assume a 0% failure probability for BGH, given the large number of outages with missing component grouping information. As a compromise, the failure probabilities output by the AGH model were taken to represent overall “Hardware” failure probabilities and used for BGH as well. The failure probabilities for AGH and BGH were then processed according to their proper component groupings downstream of the BU model.

This change also required a modification to the manner in which structure-days are calculated. Previously, every structure along the line was counted when fitting the model. However,

structures do not include components of every component grouping. For example, a structure that is a wood pole cannot also be a steel structure. This means that when estimating the failure probabilities of wood poles on an ETL, it is important to note both the number of failures attributable to wood poles (discussed previously) and the number of wood poles that could have failed.

The 2024 update to the BU model uses component count data to address this change. For each structure, data about the component groupings present on the structure is recorded. The component-grouping models then use total component counts rather than total structure counts to estimate component-grouping-specific failure probabilities.

# 10. An Example: Wood Pole Decay

The following is an example calculation using the TCM framework to estimate the single hazard, component grouping-level, annual probability of failure for a wood pole subject to wind. The threats of wood decay and Cellon treatment are considered. For illustration purposes, results are combined across multiple hazards and multiple component groupings.

# Example Calculation for TCM Framework Overview

## *Asset identifying information*

| | |
|---|---|
| ETL: | 2060 Fort Bragg-Elk |
| Structure number: | 016/003 |
| Voltage class: | 60 |
| Equipment number: | 40666507 |
| Structure type: | ST := "wood" |
| Latitude/Longitude: | 39.334448828329499/-123.798414308094 |
| HFTD: | Tier 2 |

## *Age, condition, threat, and outage history information*

Structure age (years): $T := 63 \cdot yr$

Outstanding tag remaining strength equivalent: $SdS_{0.tag} := 1$ (no outstanding tags)

PT&T current remaining strength: $SdS_{0.PTT} := 0.772813927092266$

PT&T decay rate (strength loss per year): $k_D := \frac{-0.0132767541007279}{yr}$

Combined remaining strength:

$$SdS_0 := 1 - \sqrt{\left(1 - SdS_{0.tag}\right)^2 + \left(1 - SdS_{0.PTT}\right)^2} \qquad \boxed{SdS_0 = 0.773}$$

Cellon treatment?: Cellon := "Y"

Design life reduction factor for Cellon treatment:

$$DLRF_{CT} := \begin{cases} \frac{1}{3} & \text{if Cellon = "Y"} \\ 0 & \text{otherwise} \end{cases} \qquad \boxed{DLRF_{CT} = 0.333}$$

Bayesian adjustment to median and beta: $\delta_{med} := -35.3mph$ $\delta_{beta} := 0.009$

## *Fragility function*

Initial median and uncertainty:

$$\mu_{new} := \begin{cases} 163.940459 & \text{if } ST = \text{"steel "} \\ 169.57949 & \text{otherwise} \end{cases} \cdot mph \qquad \beta_{new} := \begin{cases} 0.2 & \text{if } ST = \text{"steel"} \\ 0.3 & \text{otherwise} \end{cases}$$

$\mu_{new} = 169.579 \cdot mph$ $\beta_{new} = 0.3$

"No threat" design life: $t_D := 150 \cdot yr$

Uncertainty at design life:

$$\beta_D := \begin{cases} 0.246529291 & \text{if } ST = \text{"steel"} \\ 0.367186527 & \text{otherwise} \end{cases}$$

$\beta_D = 0.367$

PLSCADD location ratio: $V_{LR} := 1.4142$

Median adjustment for threat:

Current median: $\mu_0 := \sqrt{SdS_0} \cdot V_{LR} \cdot (\mu_{new} + \delta_{med})$ $\mu_0 = 166.939 \cdot mph$

Forecast median in "$t_F$" years, considering threat: $\mu_F(t_F) := \max\left[0, \sqrt{SdS_0 + k_D \cdot t_F} \cdot V_{LR} \cdot (\mu_{new} + \delta_{med})\right]$

Uncertainty adjustment for threat:

Adjusted design life: $t_{adj} := (1 - DLRF_{CT}) \cdot t_D$ $t_{adj} = 100 \cdot yr$

Current uncertainty: $\beta_0 := (\beta_{new} + \delta_{beta}) + (\beta_D - \beta_{new}) \cdot \left(\frac{T}{t_{adj}}\right)^2$ $\beta_0 = 0.336$

Forecast uncertainty in "$t_F$" years: $\beta_F(t_F) := (\beta_{new} + \delta_{beta}) + (\beta_D - \beta_{new}) \cdot \left(\frac{T + t_F}{t_{adj}}\right)^2$

### *Plot of fragility*

New fragility function: $f_{new}(V) := plnorm\left(\frac{V}{mph}, ln\left(\frac{\mu_{new}}{mph}\right), \beta_{new}\right)$

Current fragility function: $f_0(V) := plnorm\left(\frac{V}{mph}, ln\left(\frac{\mu_0}{mph}\right), \beta_0\right)$

Forecast fragility function in "$t_F$" years: $f_F(V, t_F) := plnorm\left(\frac{V}{mph}, ln\left(\frac{\mu_F(t_F)}{mph}\right), \beta_F(t_F)\right)$

Plot variable: $V_{plot} := 1 \cdot mph, 2 \cdot mph .. 4\mu_0$

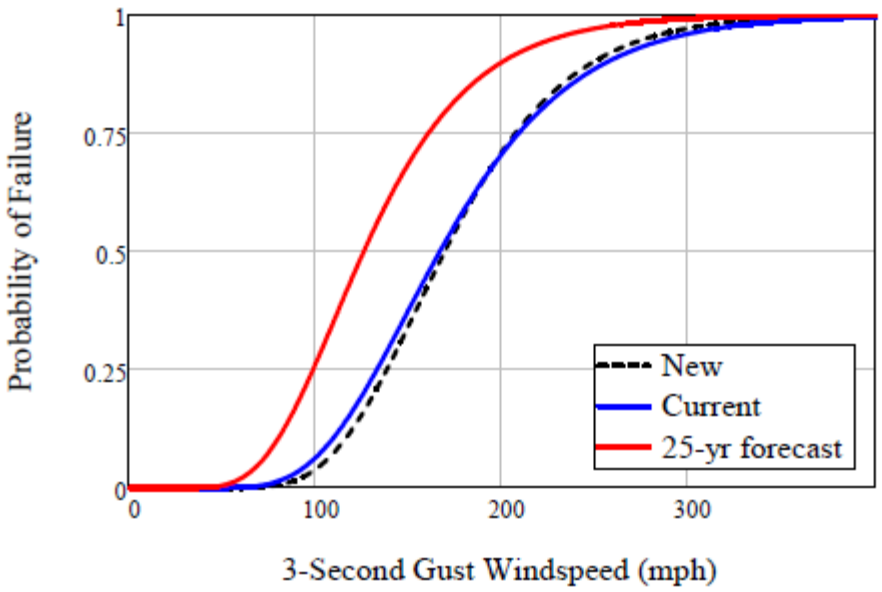

## *Hazard curve*

POMMS grid cell: 80_314

Gumbel fit (proportion of days when gust is not exceeded):

$m := 14.71849113 \cdot mph$ $s := 4.488826891 \cdot mph$ $Fit(V) := e^{-e^{\frac{-(V-m)}{s}}}$

Hazard curve: $H(V) := 365(1 - Fit(V))$

## *Plot of hazard curve*

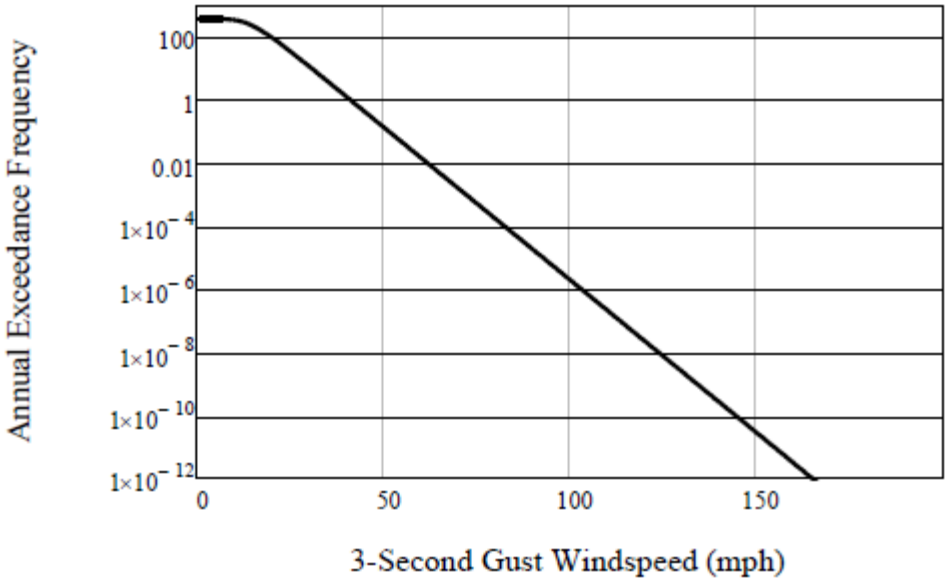

### *Risk integral*

Annual failure rate:

New condition: $\lambda_{new} := \int_0^{300mph} f_{new}(V) \cdot \left| \frac{d}{dV} H(V) \right| dV$

Current condition: $\lambda_0 := \int_0^{300mph} f_0(V) \cdot \left| \frac{d}{dV} H(V) \right| dV$

Forecast condition in "t" years: $\lambda_F(t) := \int_0^{300mph} f_F(V,t) \cdot \left| \frac{d}{dV} H(V) \right| dV$

Annual probability of failure:

New condition: $P_{f\_new} := 1 - e^{-\lambda_{new}}$ $\boxed{P_{f\_new} = 2.771 \times 10^{-5}}$

Current condition: $P_{f\_0} := 1 - e^{-\lambda_0}$ $\boxed{P_{f\_0} = 1.494 \times 10^{-4}}$

Forecast condition in "t" years: $P_{f\_F}(t) := 1 - e^{-\lambda_F(t)}$

Forecast condition in 25 years: $\boxed{P_{f\_F}(25yr) = 5.602 \times 10^{-3}}$

***Risk integral (continued)***

Calculate "no-observed decay or tag" annual probability of failure for comparison purposes

Forecast fragility function in "$t_F$" years,
no observed decay or tag:

$$f_{F\_NT}(V, t_F) := \text{plnorm}\left[\frac{V}{\text{mph}}, \ln\left[\frac{V_{LR}\cdot(\mu_{new} + \delta_{med})}{\text{mph}}\right], \beta_F(t_F)\right]$$

Forecast condition in "t" years,
no observed decay or tag:

$$\lambda_{F\_NT}(t) := \int_0^{300\text{mph}} f_{F\_NT}(V, t)\cdot\left|\frac{d}{dV}H(V)\right| dV$$

$$P_{f\_F\_NT}(t) := 1 - e^{-\lambda_{F\_NT}(t)}$$

Plot variable:

$$t_{plot} := 0, 5\text{yr}.. 1.5t_D$$

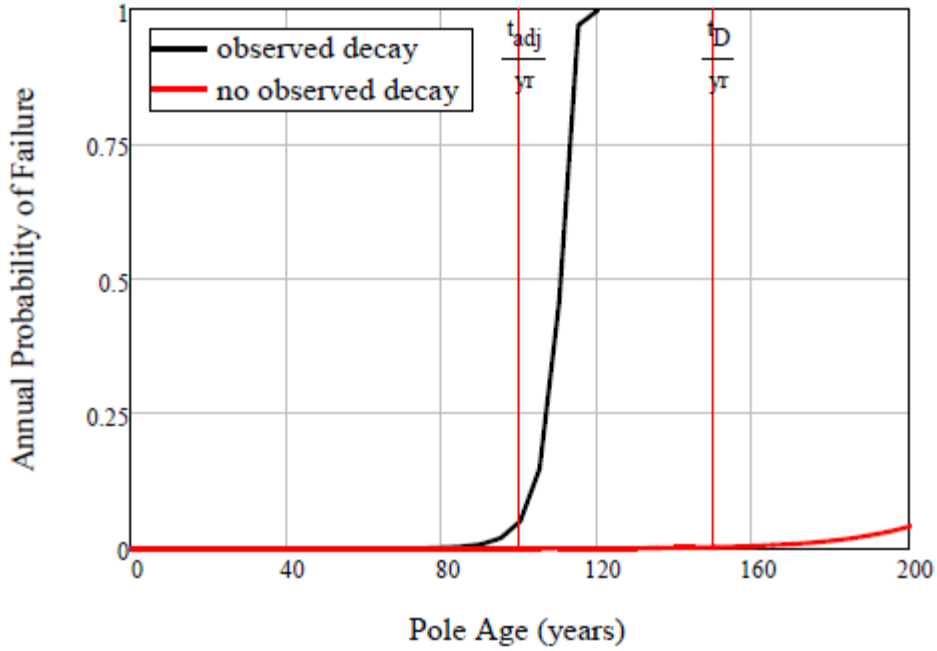

### *Combining annual probabilities of failure*

For illustration purposes, the results above are combined with the following hazards and component groupings:

Wind hazard (applies to all component groupings present)

$$\lambda_w := \begin{pmatrix} \lambda_0 \\ 0.000170 \\ 0.000211 \\ 0.000526 \\ 0.000115 \\ 0.000115 \end{pmatrix}$$

-wood structure
-conductor
-insulator
-splice
-above grade hardware
-below grade hardware

$$Pf_w := 1 - e^{-\lambda_w} \qquad Pf_w = \begin{pmatrix} 1.494 \times 10^{-4} \\ 1.7 \times 10^{-4} \\ 2.11 \times 10^{-4} \\ 5.259 \times 10^{-4} \\ 1.15 \times 10^{-4} \\ 1.15 \times 10^{-4} \end{pmatrix}$$

Seismic hazard (applies only to wood structure component grouping)

$$\lambda_s := \begin{pmatrix} 0.0000173 \\ 0 \\ 0 \\ 0 \\ 0 \\ 0 \end{pmatrix}$$

-wood structure
-conductor
-insulator
-splice
-above grade hardware
-below grade hardware

$$Pf_s := 1 - e^{-\lambda_s} \qquad Pf_s = \begin{pmatrix} 1.73 \times 10^{-5} \\ 0 \\ 0 \\ 0 \\ 0 \\ 0 \end{pmatrix}$$

***Combining annual probabilities of failure (continued)***

Other hazards (ML models, apply only to specific component groupings)

Balloon: $\lambda_{ba} := \begin{pmatrix} 0 \\ 0.000207 \\ 0 \\ 0 \\ 0 \\ 0 \end{pmatrix}$ $Pf_{ba} := 1 - e^{-\lambda_{ba}}$ $Pf_{ba} = \begin{pmatrix} 0 \\ 2.07 \times 10^{-4} \\ 0 \\ 0 \\ 0 \\ 0 \end{pmatrix}$

Car strike: $\lambda_{cs} := \begin{pmatrix} 0.0000980 \\ 0 \\ 0 \\ 0 \\ 0 \\ 0 \end{pmatrix}$ $Pf_{cs} := 1 - e^{-\lambda_{cs}}$ $Pf_{cs} = \begin{pmatrix} 9.8 \times 10^{-5} \\ 0 \\ 0 \\ 0 \\ 0 \\ 0 \end{pmatrix}$

Gunshot: $\lambda_{gs} := \begin{pmatrix} 0 \\ 0.0000191 \\ 0.0000191 \\ 0 \\ 0 \\ 0 \end{pmatrix}$ $Pf_{gs} := 1 - e^{-\lambda_{gs}}$ $Pf_{gs} = \begin{pmatrix} 0 \\ 1.91 \times 10^{-5} \\ 1.91 \times 10^{-5} \\ 0 \\ 0 \\ 0 \end{pmatrix}$

Bird strike: $\lambda_{bs} := \begin{pmatrix} 0.00000384 \\ 0.00000384 \\ 0 \\ 0 \\ 0 \\ 0 \end{pmatrix}$ $Pf_{bs} := 1 - e^{-\lambda_{bs}}$ $Pf_{bs} = \begin{pmatrix} 3.84 \times 10^{-6} \\ 3.84 \times 10^{-6} \\ 0 \\ 0 \\ 0 \\ 0 \end{pmatrix}$

Vegetation: $\lambda_{vg} := \begin{pmatrix} 0.00529 \\ 0.00529 \\ 0 \\ 0 \\ 0 \\ 0 \end{pmatrix}$ $Pf_{vg} := 1 - e^{-\lambda_{vg}}$ $Pf_{vg} = \begin{pmatrix} 5.276 \times 10^{-3} \\ 5.276 \times 10^{-3} \\ 0 \\ 0 \\ 0 \\ 0 \end{pmatrix}$

### *Combining annual probabilities of failure (continued)*

Single hazard, asset-level, annual probability of failure

Wind:

$$Pf_{w\_asset\_ind} := 1 - \prod_{i=1}^{length(\lambda_w)} \left(1 - Pf_{w_i}\right) \qquad Pf_{w\_asset\_ind} = 1.286 \times 10^{-3}$$

$$Pf_{w\_asset\_dep} := \max\left(Pf_w\right) \qquad Pf_{w\_asset\_dep} = 5.259 \times 10^{-4}$$

$$Pf_{w\_asset} := mean\left(Pf_{w\_asset\_ind}, Pf_{w\_asset\_dep}\right) \qquad \boxed{Pf_{w\_asset} = 9.057 \times 10^{-4}}$$

Seismic:

$$Pf_{s\_asset\_ind} := 1 - \prod_{i=1}^{length(\lambda_s)} \left(1 - Pf_{s_i}\right) \qquad Pf_{s\_asset\_ind} = 1.73 \times 10^{-5}$$

$$Pf_{s\_asset\_dep} := \max\left(Pf_s\right) \qquad Pf_{s\_asset\_dep} = 1.73 \times 10^{-5}$$

$$Pf_{s\_asset} := mean\left(Pf_{s\_asset\_ind}, Pf_{s\_asset\_dep}\right) \qquad \boxed{Pf_{s\_asset} = 1.73 \times 10^{-5}}$$

Balloon:

$$Pf_{ba\_asset\_ind} := 1 - \prod_{i=1}^{length(\lambda_{ba})} \left(1 - Pf_{ba_i}\right) \qquad Pf_{ba\_asset\_ind} = 2.07 \times 10^{-4}$$

$$Pf_{ba\_asset\_dep} := \max\left(Pf_{ba}\right) \qquad Pf_{ba\_asset\_dep} = 2.07 \times 10^{-4}$$

$$Pf_{ba\_asset} := mean\left(Pf_{ba\_asset\_ind}, Pf_{ba\_asset\_dep}\right) \qquad \boxed{Pf_{ba\_asset} = 2.07 \times 10^{-4}}$$

Car strike:

$$Pf_{cs\_asset\_ind} := 1 - \prod_{i=1}^{length(\lambda_{cs})} \left(1 - Pf_{cs_i}\right) \qquad Pf_{cs\_asset\_ind} = 9.8 \times 10^{-5}$$

$$Pf_{cs\_asset\_dep} := \max\left(Pf_{cs}\right) \qquad Pf_{cs\_asset\_dep} = 9.8 \times 10^{-5}$$

$$Pf_{cs\_asset} := mean\left(Pf_{cs\_asset\_ind}, Pf_{cs\_asset\_dep}\right) \qquad \boxed{Pf_{cs\_asset} = 9.8 \times 10^{-5}}$$

### *Combining annual probabilities of failure (continued)*

Single hazard, asset-level, annual probability of failure (continued)

Gunshot:

$$Pf_{gs\_asset\_ind} := 1 - \prod_{i=1}^{length(\lambda_{gs})} \left(1 - Pf_{gs_i}\right) \qquad Pf_{gs\_asset\_ind} = 3.82 \times 10^{-5}$$

$$Pf_{gs\_asset\_dep} := \max\left(Pf_{gs}\right) \qquad Pf_{gs\_asset\_dep} = 1.91 \times 10^{-5}$$

$$Pf_{gs\_asset} := mean\left(Pf_{gs\_asset\_ind}, Pf_{gs\_asset\_dep}\right) \qquad \boxed{Pf_{gs\_asset} = 2.865 \times 10^{-5}}$$

Bird strike:

$$Pf_{bs\_asset\_ind} := 1 - \prod_{i=1}^{length(\lambda_{bs})} \left(1 - Pf_{bs_i}\right) \qquad Pf_{bs\_asset\_ind} = 7.68 \times 10^{-6}$$

$$Pf_{bs\_asset\_dep} := \max\left(Pf_{bs}\right) \qquad Pf_{bs\_asset\_dep} = 3.84 \times 10^{-6}$$

$$Pf_{bs\_asset} := mean\left(Pf_{bs\_asset\_ind}, Pf_{bs\_asset\_dep}\right) \qquad \boxed{Pf_{bs\_asset} = 5.76 \times 10^{-6}}$$

Vegetation:

$$Pf_{vg\_asset\_ind} := 1 - \prod_{i=1}^{length(\lambda_{vg})} \left(1 - Pf_{vg_i}\right) \qquad Pf_{vg\_asset\_ind} = 0.011$$

$$Pf_{vg\_asset\_dep} := \max\left(Pf_{vg}\right) \qquad Pf_{vg\_asset\_dep} = 5.276 \times 10^{-3}$$

$$Pf_{vg\_asset} := mean\left(Pf_{vg\_asset\_ind}, Pf_{vg\_asset\_dep}\right) \qquad \boxed{Pf_{vg\_asset} = 7.9 \times 10^{-3}}$$

$$Pf_{asset\_single} := \begin{pmatrix} Pf_{w\_asset} \\ Pf_{s\_asset} \\ Pf_{ba\_asset} \\ Pf_{cs\_asset} \\ Pf_{gs\_asset} \\ Pf_{bs\_asset} \\ Pf_{vg\_asset} \end{pmatrix}$$

### *Combining annual probabilities of failure (continued)*

Multi-hazard, component group-level, annual probability of failure

$$\lambda_{multi} := \lambda_w + \lambda_s + \lambda_{ba} + \lambda_{cs} + \lambda_{gs} + \lambda_{bs} + \lambda_{vg}$$

$$Pf_{multi} := 1 - e^{-\lambda_{multi}}$$

$$Pf_{multi} = \begin{pmatrix} 5.543 \times 10^{-3} \\ 5.674 \times 10^{-3} \\ 2.301 \times 10^{-4} \\ 5.259 \times 10^{-4} \\ 1.15 \times 10^{-4} \\ 1.15 \times 10^{-4} \end{pmatrix}$$

-wood structure
-conductor
-insulator
-splice
-above grade hardware
-below grade hardware

Multi-hazard, asset-level, annual probability of failure

$$Pf_{asset\_multi} := 1 - \prod_{i=1}^{rows(Pf_{asset\_single})} \left(1 - Pf_{asset\_single_i}\right)$$

$$Pf_{asset\_multi} = 9.152 \times 10^{-3}$$

# Appendix A

# Seismic Hazard Models

# Appendix B

# Wood Decay Model

# Appendix C

# Cellon Gas Preservative Treatment in the TCM

# Appendix D

# Atmospheric Corrosion Models

# Appendix E

# Underground Corrosion Models

# Appendix F

# Aeolian Vibration Model

# Appendix G

# Wear Model

# Appendix H

# Insulator Contamination Model (In Progress)

# Appendix I

# Polymer Insulator Aging Model